SOLUTION TO THE BINARY DIFFUSION LAMINAR BOUNDARY LAYER EQUATIONS INCLUDING THE EFFECT OF SECOND-ORDER TRANSVERSE CURVATURE

N. A. Jaffe, R. C. Lind, and A. M. O. Smith
Douglas Aircraft Division
a Division of Douglas Aircraft Company, Inc.
Long Beach, California

February 1967

ARNOLD ENGINEERING DEVELOPMENT CENTER
AIR FORCE SYSTEMS COMMAND
ARNOLD AIR FORCE STATION, TENNESSEE

NOTICES

When U. S. Government drawings specifications, or other data are used for any purpose other than a definitely related Government procurement operation, the Government thereby incurs no responsibility nor any obligation whatsoever, and the fact that the Government may have formulated, furnished, or in any way supplied the said drawings, specifications or other data, is not to be regarded by implication or otherwise, or in any manner licensing the holder or any other person or corporation, or conveying any rights or permission to manufacture, use, or sell any patented invention that may in any way be related thereto.

Qualified users may obtain copies of this report from the Defense Documentation Center.

References to named commercial products in this report are not to be considered in any sense as an endorsement of the product by the United States Air Force or the Government.

SOLUTION TO THE BINARY DIFFUSION LAMINAR BOUNDARY LAYER EQUATIONS INCLUDING THE EFFECT OF SECOND-ORDER TRANSVERSE CURVATURE

N. A. Jaffe, R. C. Lind, and A. M. O. Smith
Douglas Aircraft Division
a Division of Douglas Aircraft Company, Inc.
Long Beach, California

AF - AEDC
Arnold AFS Tenn

FOREWORD

The research reported herein was sponsored by the Arnold Engineering Development Center, Air Force Systems Command, under Program Element 62405334, Project 8953, Task 895303 and 895306. The work was performed by Douglas Aircraft Division, a division of Douglas Aircraft Company, Inc., Long Beach, California, under Purchase Order 5A-9405 that was made under the provisions of Prime Contract AF40(600)-1000 between the U. S. Air Force and ARO, Inc. (a subsidiary of Sverdrup & Parcel and Associates, Inc.), operating contractor of AEDC, AFSC, Arnold Air Force Station, Tennessee.

The reproducibles supplied by the authors were used in the reproduction of this report. The Douglas Aircraft Division report number is LB 32613.

The authors express their gratitude to Mr. Donald Baron for his painstaking efforts in programming the equations. In addition, Mr. David Callin is acknowledged for checking many of the numerical results.

This technical report has been reviewed and is approved.

Carl E. Simmons	Edward R. Feicht
Captain, USAF	Colonel, USAF
Directorate of Plans and Technology	Director of Plans and Technology

1.0 SUMMARY

This report presents a numerical method for solving the binary diffusion laminar boundary-layer equations. The differential equations of continuity, momentum, energy, and species diffusion are solved simultaneously for two-dimensional or axisymmetric flow. For the case of axisymmetric flow the second-order transverse curvature terms appearing in the equations are retained.

Relations for mixture fluid properties as functions of local conditions in the boundary layer are developed and used in obtaining solutions to the equations. The mixtures considered in this investigation are He - air, Ar - air, and CO_2 - air.

Solutions to the equations are given for flow of a pure air free stream over a 9° half angle cone at a free stream Mach number of 10 and free stream Reynolds number, based on cone slant length of 940. The initial section of the cone is solid and mass injection is initiated at a location downstream of the tip. Results are presented and compared for calculations both including and neglecting the second-order transverse curvature effect.

2.0 TABLE OF CONTENTS

3.0 INDEX OF FIGURES

4.0 NOMENCLATURE

C	$\rho\mu / \rho_e \mu_e$
C_p	constant pressure specific heat of mixture
C_{p_f}	constant pressure specific heat of species f
C_V	constant volume specific heat of mixture
C_{V_f}	constant volume specific heat of species f
c_f	mass fraction of free stream species, ρ_f / ρ
c_i	mass fraction of injected species, ρ_i / ρ
D_f^T	thermal coefficient of diffusion
D_{fi}	binary diffusion coefficient
f	stream function (equation 16)
g	dimensionless enthalpy ratio H/He
H	total specific enthalpy of mixture
h	static specific enthalpy of mixture
h_f	static specific enthalpy of species f
K_1	bound on trial solutions of momentum equation
K_2	bound on trial solutions of energy equation
k	Boltzmann constant
L	reference body length
Le	Lewis number $\rho D_{fi} C_p / \lambda$
M_f	molecular weight of species f
M_{fi}	reduced molecular weight of species f and i
n	count of successive steps in transformed x direction

p	pressure
Pr	Prandtl number $\mu C_p/\lambda$
R'	universal gas constant
r	distance from axis of symmetry to location in the boundary layer
S	dimensionless concentration parameter (see equation 27)
T	temperature
t	transverse curvature parameter (see equation 25)
u	velocity component in x direction
v	velocity component in y direction
$\bar{v}$	transformed velocity (equation 8)
X_f	mole fraction of species f
x	direction along surface measured from leading edge or stagnation point
y	direction measured normal to surface
z	mass fraction ratio c_f/c_{f_e}
β	dimensionless velocity gradient (see equation 26)
ϵ_1	convergence criterion for momentum equation
ϵ_2	convergence criterion for energy equation
ϵ_3	perturbation of initial condition on energy equation
$\bar{\eta},\eta$	transformed y coordinate
η_∞	maximum value of η used in numerical solution
λ	thermal conductivity of mixture
λ_f	thermal conductivity of species f
μ	viscosity of mixture
μ_f	viscosity of species f

ρ mass density of mixture

$\bar{\xi}, \xi$ transformed x coordinate

SUBSCRIPTS

e evaluated at edge of boundary layer

f evaluated for species f

i evaluated for species i

n evaluated at station n

w evaluated at surface

∞ evaluated at free stream conditions or see η_∞

Primed quantities denote differentation with respect to η or $\bar{\eta}$; barred quantities refer to variables based upon transformation given by equations (6), (7), and (14), (15).

5.0 INTRODUCTION

This report describes a general method for solving the laminar diffusion boundary-layer equations for a binary gas mixture. The primary object of this investigation has been the development of an exact method of solution to the governing flow equations applicable to arbitrary two-dimensional or axisymmetric shapes and a wide range of flow conditions, such as might be incurred during wind tunnel tests or actual flight conditions.

Significant contributions, which are briefly reviewed here, to the field of analysis of the binary diffusion laminar boundary-layer equations have been made by Baron, Covert, Culick, and co-workers at MIT. Baron (reference 1) developed the basic equations describing the binary mixture laminar boundary layer and solved them for the case of similar flows with zero pressure gradient, solutions were given for Schmidt number and Prandtl number of unity. An integral method was used to obtain the effect of mass transfer downstream of the injection point. Cases were computed for injection of helium and carbon dioxide into air. Covert (reference 2) developed an approximate integral method, valid for small injection rates, which could be employed without the use of large scale computers. Baron and Scott (reference 3) extended the analysis to flows with pressure gradients; this study was restricted to similar flows. Cases were computed for injection of helium over a temperature range for which the vibrational relaxation contribution to the heat capacity was neglected. A more general analysis of the problem (viz. not restricted to similar flows) was made by Moran and Scott

(reference 4). The equations were solved in terms of Crocco variables using a finite-difference technique developed by Flügge-Lotz and Baxter (reference 5). The method requires starting profiles and is apparently not capable of handling large changes taking place in the streamwise direction. Again a helium - air mixture was considered over a temperature range for which vibrational relaxation of the air molecules could be ignored. Covert's method was extended by Moran (reference 6) to flows over a porous cone with solid tip. In reference (7) Culick developed an integral method to solve the diffusion equation for zero pressure gradient flows. Velocity and enthalpy profiles are required for this method which was applied to flows with helium injection into air. Subsequently, Culick (reference 8) developed a method for zero pressure gradient flows. This is also an integral method. It utilizes integral relations between heat and surface mass transfer and does not require a previously obtained solution to the energy equation. Results are presented for both helium and air injection.

The previous studies were primarily concerned with the application of mass injection for cooling; moreover, the second-order transverse curvature terms for axisymmetric flow were not included in the equations. Recent experimental measurements with mass injection of helium and air into air (references 9 and 10) in hypersonic flow over slender cones indicates that mass injection has a marked effect on drag coefficients as well as heat transfer. The results reported in references (9) and (10) were for low Reynolds number flows and the total drag was predominantly skin friction drag. Hence, it is to be expected that solutions to the boundary-layer equations for flows with mass transfer will prove valuable for the

prediction of the effects of mass injection on drag coefficients in certain flight regimes. In addition, results reported in references (9), (10), and (11), which were based upon measurements for hypersonic flow over slender cones, indicate that the transverse curvature effect may be significant. The theoretical methods used to treat this effect in the above references were not exact; hence, to gain more insight into the problem, the second-order transverse curvature terms appearing in the boundary layer equations have been retained in the present investigation.

A numerical method based on ideas originated by Hartree and Womersley (reference 12) is used to solve the flow equations. The method has been developed for solution of the incompressible laminar boundary-layer equations (reference 13), the compressible laminar boundary-layer equations (reference 14), and the laminar boundary-layer equations of a binary nonequilibrium dissociating gas (reference 15). The primary differences between the work described in this report and that described in reference (15) are the mathematical transformations used and the mixture fluid properties incorporated in the computer program. The computer program developed makes it possible to include or neglect the second-order transverse curvature terms appearing in the equations.

Numerical results for injection of helium, argon, and air into air for flow over a 9° half-angle cone at a Mach number of 10 and free-stream Reynolds number based on slant length are given. The free stream conditions are within the range of test conditions of the AEDC-VKF Low Density Tunnel L.

6.0 ANALYSIS

6.1 Basic Equations

The laminar boundary-layer of a binary gas mixture with no chemical reactions is considered for two-dimensional or axisymmetric flow. The actual mixtures studied are: He - air, Ar - air, and CO_2 - air. Although thermal diffusion is neglected in the numerical calculations it is retained in the development of the equations. The second-order transverse curvature terms are retained and handled through use of a transformation introduced by Probstein and Elliott (reference 16.) The equations are further transformed to the form in which they are finally solved through use of the Levy - Lees transformation (reference 17). The final equations resulting from the combined Probstein-Elliott and Levy-Lees transformations contain a common term and it is shown that neglect of this term reduces the equations to the standard two-dimensional or axisymmetric form.

The equations containing transverse curvature in a curvilinear coordinate system are as follows:

Overall Continuity

$$\frac{\partial}{\partial x}\,(r\rho u) + \frac{\partial}{\partial y}\,(r\rho v) = 0 \qquad (1)$$

Momentum

$$\rho\left(u\,\frac{\partial u}{\partial x} + v\,\frac{\partial u}{\partial y}\right) = -\frac{dp}{dx} + \frac{1}{r}\,\frac{\partial}{\partial y}\left(r\mu\,\frac{\partial u}{\partial y}\right) \qquad (2)$$

Energy

$$\rho\left(u\,\frac{\partial H}{\partial x}+v\,\frac{\partial H}{\partial y}\right)=\frac{1}{r}\frac{\partial}{\partial y}\left\{r\left[\frac{\mu}{Pr}\,\frac{\partial H}{\partial y}+\mu\left(1-\frac{1}{Pr}\right)u\,\frac{\partial u}{\partial y}\right]\right\}$$

$$+\frac{1}{r}\,\frac{\partial}{\partial y}\left\{r\left[\frac{\mu}{Pr}(Le-1)\,(h_f-h_i)\frac{\partial c_f}{\partial y}+D_f^T\,(h_f-h_i)\,\frac{1}{T}\,\frac{\partial T}{\partial y}\right]\right\} \quad (3)$$

Species

$$\rho\left(u\,\frac{\partial c_f}{\partial x}+v\,\frac{\partial c_f}{\partial y}\right)=\frac{1}{r}\frac{\partial}{\partial y}\left[r\left(\rho D_{fi}\,\frac{\partial c_f}{\partial y}+\frac{D_f^T}{T}\,\frac{\partial T}{\partial y}\right)\right] \quad (4)$$

6.2 Transformed Equations

For axisymmetric flow a position in the boundary layer is determined by specifying the coordinates x, y, and r (see Figure 1) where r is given by

$$r\,(x, y) = r_o\,(x) + y\cos\alpha \quad (5)$$

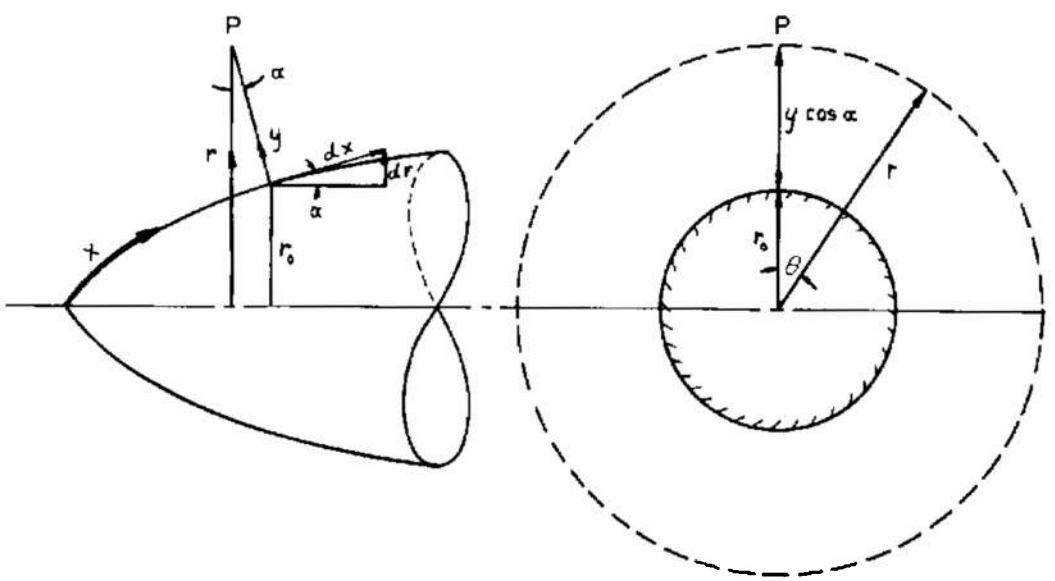

Figure 1. Coordinates for Axially Symmetric Body

The body shape is specified by the function $r_o(x)$. Equations (1) thru (4) can be placed in an almost two-dimensional form through use of the following transformation originated by Probstein and Elliott (reference 16).

$$l\bar{y} = (r(x, y)/L)\, dy \tag{6}$$

$$a\bar{x} = (r_o(x)/L)^2\, dx \tag{7}$$

This differs from the Mangler transformation in that r (x, y) appears in equation (6) rather than $r_o(x)$. Moreover, the Mangler transformation is normally applied only to the boundary layer equations containing the first order transverse curvature term. The y velocity component v is eliminated through the following relation

$$\bar{v} = \left(\frac{rL}{r_o^2}\right)v + \left[\left(\frac{L}{r_o}\right)^2\left(\frac{\partial \bar{y}}{\partial x}\right)\right]u \tag{8}$$

Equations (1) thru (4) in the new coordinate system and in terms of $\bar{v}$ become

Continuity

$$\frac{\partial}{\partial \bar{x}}(\rho u) + \frac{\partial}{\partial \bar{y}}(\rho \bar{v}) = 0 \tag{9}$$

Momentum

$$\rho\left(u\frac{\partial u}{\partial \bar{x}} + \bar{v}\frac{\partial u}{\partial \bar{y}}\right) = -\frac{dp}{d\bar{x}} + \frac{\partial}{\partial \bar{y}}\left(\mu\frac{r^2}{r_o^2}\frac{\partial u}{\partial \bar{y}}\right) \tag{10}$$

Energy

$$\rho\left(u\ \frac{\partial H}{\partial \bar{x}} + \bar{v}\ \frac{\partial H}{\partial \bar{y}}\right) = \frac{\partial}{\partial \bar{y}}\left\{\frac{r^2}{r_o^2}\left[\frac{\mu}{Pr}\ \frac{\partial H}{\partial \bar{y}} + \mu\left(1-\frac{1}{Pr}\right) u\ \frac{\partial u}{\partial \bar{y}}\right.\right.$$

$$\left.\left. + \frac{\mu}{Pr}\,(Le-1)\,(h_f - h_i)\ \frac{\partial c_f}{\partial \bar{y}} + D_f^T\,(h_f - h_i)\,\frac{1}{T}\ \frac{\partial T}{\partial \bar{y}}\right]\right\} \qquad (11)$$

Species

$$\rho\left(u\ \frac{\partial c_f}{\partial \bar{x}} + \bar{v}\ \frac{\partial c_f}{\partial \bar{y}}\right) = \frac{\partial}{\partial \bar{y}}\left\{\frac{r^2}{r_o^2}\left[\left(\rho\, D_{fi}\ \frac{\partial c_f}{\partial \bar{y}} + \frac{D_f^T}{T}\ \frac{\partial T}{\partial \bar{y}}\right)\right]\right\} \qquad (12)$$

The quantity $(r/r_o)^2$ is given by

$$\frac{r^2}{r_o^2} = 1 + \frac{2L}{r_o^2}\ \bar{y}\cos\alpha \qquad (13)$$

It can be seen that neglecting the second term on the right-hand side of equation (13) reduces equations (9) thru (12) to the two-dimensional form.

The following transformation (reference 17) is now introduced in order to place the equations in a form more suitable for solution

$$\bar{\xi} = \int_o^{\bar{x}} \rho_e\, u_e\, \mu_e\, d\bar{x} \qquad (14)$$

$$\bar{\eta} = \frac{\rho_e\ u_e}{(2\bar{\xi})^{1/2}} \int_o^{\bar{y}} \frac{\rho}{\rho_e}\ d\bar{y} \qquad (15)$$

and equations (9) and (10) are combined through use of a stream function given by

$$\bar{\psi} = (2\bar{\xi})^{1/2}\, f(\bar{x}, \bar{\eta}) \qquad (16)$$

where

$$\rho u = \frac{\partial \bar{\psi}}{\partial \bar{y}} \quad , \quad \rho \bar{v} = - \frac{\partial \bar{\psi}}{\partial \bar{x}} \tag{17}$$

The following relations are used to express the partial derivative operators in the new coordinate system

$$\left(\frac{\partial}{\partial \bar{y}}\right)_{\bar{x}} = \frac{u_e \rho}{(2\bar{\xi})^{1/2}} \left(\frac{\partial}{\partial \bar{\eta}}\right)_{\bar{\xi}} \tag{18}$$

$$\left(\frac{\partial}{\partial \bar{x}}\right)_{\bar{y}} = \rho u_e \mu_e \left[\left(\frac{\partial}{\partial \bar{\xi}}\right)_{\bar{\eta}} + \left(\frac{\partial \bar{\eta}}{\partial \bar{\xi}}\right)_{\bar{y}} \left(\frac{\partial}{\partial \bar{\eta}}\right)_{\bar{\xi}}\right] \tag{19}$$

and

$$\left(\frac{\partial \bar{\eta}}{\partial \bar{\xi}}\right)_{\bar{y}} = \frac{u_e}{(2\bar{\xi})^{1/2}} \int_0^{\bar{y}} \left(\frac{\partial \rho}{\partial \bar{\xi}}\right)_{\bar{y}} d\bar{y} - \frac{1}{2\bar{\xi}} \frac{u_e \int_0^{\bar{y}} \rho d\bar{y}}{(2\bar{\xi})^{1/2}} \tag{20}$$

From equations (16), (17), and (18) it can be shown that

$$f' = \left(\frac{\partial f}{\partial \bar{\eta}}\right)_{\bar{x}} = \frac{u}{u_e} \tag{21}$$

Introducing the stream function f, applying the above operators and non-dimensionalizing by the factor $(\bar{\xi}/\rho u_e^2)$ yields

Momentum

$$[C(1+t)\, f'']' + \beta\left(\frac{\rho_e}{\rho} - f'^2\right) + ff'' = 2\bar{\xi}\left(f' \frac{\partial f'}{\partial \bar{\xi}} - f'' \frac{\partial f}{\partial \bar{\xi}}\right) \tag{22}$$

Energy

$$\left[C\,(1+t)\left\{\frac{g'}{Pr}+\frac{u_e^2}{H_e}\left(1-\frac{1}{Pr}\right)f'\,f''+\frac{h_f-h_i}{H_e}\left(\frac{Le-1}{Pr}c_{f_e}z'+\frac{D_f^T}{\mu}\frac{T'}{T}\right)\right\}\right]'$$

$$+fg' = 2\bar{\xi}\left(f'\frac{\partial g}{\partial\bar{\xi}}-g'\frac{\partial f}{\partial\bar{\xi}}\right) \tag{23}$$

Species

$$\left[C(1+t)\left(\frac{Le}{Pr}\,z'+\frac{D_f\,T'}{c_{f_e}\,\mu\,T}\right)\right]'-Szf'+fz' = 2\bar{\xi}\left(f'\frac{\partial z}{\partial\bar{\xi}}-z'\frac{\partial f}{\partial\bar{\xi}}\right) \tag{24}$$

where

$$t = 2\sqrt{2}\;L\bar{\xi}^{1/2}\frac{\cos\alpha}{r_o^2\;\rho_e u_e}\int_o^{\bar{y}}\frac{\rho_e}{\rho}\,d\bar{y} \tag{25}$$

$$\beta = \frac{2\bar{\xi}}{u_e}\;\frac{du_e}{d\bar{\xi}} \tag{26}$$

$$S = 2\,\frac{\bar{\xi}}{c_{f_e}}\;\frac{dc_{f_e}}{d\bar{\xi}} \tag{27}$$

$$g = H/He \tag{28}$$

$$z = c_f/c_{f_e} \tag{29}$$

The boundary conditions on equations (22) - (24) are:

$\bar{\eta} = 0$:

$$f = \frac{-1}{(2\bar{\xi})^{1/2}}\int_o^{\bar{x}}\rho_w\,v_w\left(\frac{L}{r_o}\right)d\bar{x} \tag{30a}$$

$$f' = 0 \tag{30b}$$

$$\left\{\begin{array}{l} g = g_w \\ \text{or} \\ g' = g'_w \end{array}\right\} \tag{30c}$$

$$\left\{\begin{array}{l} z = z_w \\ \text{or} \\ z' = z'_w \end{array}\right\} \tag{30d}$$

$\bar{\eta} \rightarrow \infty$:

$$f' \rightarrow 1 \tag{30e}$$

$$g \rightarrow 1 \tag{30f}$$

$$z \rightarrow 1 \tag{30g}$$

It can be seen that neglect of the quantity t in equations (22) - (24) leads to the standard two-dimensional form of the laminar boundary-layer equations in the Levy - Lees coordinate system. Hence with t set equal to zero the appropriate transformation is

$$\xi = \int_o^x \rho_e \, u_e \, \mu_e \, r_o^{2k} \, dx \tag{31}$$

$$\eta = \frac{\rho_e \, u_e}{(2\xi)^{1/2}} \int_o^y r_o^k \, \frac{\rho}{\rho_e} \, dy \tag{32}$$

where k = 0 for two-dimensional flow and k = 1 for axisymmetric flow. The quantity r_o does not appear in equations (14) and (15) since it is already contained in the quantities $\bar{x}$ and $\bar{y}$. The second-order transverse curvature effects can now either be accounted for or neglected; with t given by equation (25) and application of the transformation given by equations (14) and (15) it is accounted for and with t equal to zero and application of the transformations

given by equations (31) and (32) second-order transverse curvature is not accounted for. In addition, it should be kept in mind that when t is zero and equations (31) and (32) are applied the quantity r(x, y) in the original equations (1) - (4) is replaced by r_o (x).

The equations were programmed so that transverse curvature (TVC) effects could be included or neglected in any given calculation. If TVC is neglected it is understood that the unbarred variables apply. The expressions for certain quantities such as displacement thickness and the inverse transformation back to the physical plane depend on whether the barred (including TVC) or unbarred system (neglecting TVC) is used. These expressions for both systems are developed in Section 6.5.

In order to make the solution of equations (22) - (24) possible, expressions for the fluid properties appearing in these equations are necessary.

6.3 Fluid Properties

The fluid properties developed in this section are those dealing with a binary mixture of non-reacting gases. The basic binary mixture is obtained by the injection of a foreign gas, either helium, argon, or carbon dioxide into a free stream consisting of air. The mixture properties employed in this development are functions of the mass fractions of the individual species and properties of the pure species comprising the mixture. In a binary mixture, one of the mass fractions can be eliminated by the relationship

$$c_i + c_f = 1 \tag{33}$$

The mass fraction c_i has been eliminated in the present formulation. The species equation variable z then becomes (as shown in equation (29))

$$z = \frac{c_f}{c_{f_e}} \tag{34}$$

If the free stream is uncontaminated, c_{f_e} will be one at the edge of the boundary layer, and if a foreign gas alone is injected into the boundary layer, z will be zero at the wall.

The fluid properties needed to solve the laminar boundary-layer equations of a binary mixture are: C_p, C_V, C_{p_i}, C_{p_f}, C_{V_i}, C_{V_f}, h, h_i, h_f, λ, λ_i, λ_f, μ, μ_i, μ_f, D_{fi}, D_f^T and certain combinations of these that give the dimensionless parameters Pr and Le. Storage for the coefficient

of thermal diffusion D_f^T is allocated although a numerical statement of it is not included. The fluid properties are valid in the temperature range from 50°K to 3500°K (except for C_p, which is valid to 0°K).

6.3.1 Thermodynamic Properties

The individual species comprising the gas mixture are assumed perfect but not necessarily calorically perfect. That is, the specific enthalpies of the pure species are not constant but are taken as functions only of temperature. Also the total pressure is the sum of the partial pressures of the individual species. The expression for the density ρ of a mixture of perfect gases is given by

$$\rho = \frac{p}{R'T}\left[\frac{M_i M_f}{c_f(M_i - M_f) + M_f}\right]\frac{\text{slugs}}{\text{ft}^3} \tag{35}$$

Where

$$M_f = M_{air} = 28.966$$

$$M_i = M_{Ar} = 39.948$$

$$M_{He} = 4.0083$$

$$M_{CO_2} = 44.011$$

The constant volume and constant pressure heat capacities of the mixture are given by

$$C_V = (1 - c_f)\, C_{V_i} + c_f\, C_{V_f} \tag{36}$$

and

$$C_p = (1 - c_f)\, C_{p_i} + c_f\, C_{p_f} \tag{37}$$

The constant volume heat capacities of the pure species are obtained from statistical mechanical considerations (reference 18). The modes of energy distribution considered are translation, rotation, and vibration.

For the monatomic gases, He and Ar, the translational mode is fully excited at room temperature to give the value

$$C_{V_j} = \frac{3}{2} \frac{R'}{M_j} \tag{38}$$

and there are no contributions due to rotation and vibration. For air the rotational and vibrational modes must also be used. The contribution of electronic excitations to the heat capacities are negligible in the temperature range of interest and have been neglected. The constant pressure heat capacities of He, Ar, and air are obtained by means of

$$C_{p_j} = C_{V_j} + \frac{R'}{M_j} \tag{39}$$

The constant pressure heat capacity for CO_2 was obtained from the Janaf Thermochemical Data Tables (reference 19). The C_{p_j} data for air and CO_2 have been fit to polynomials of the form

$$C_{p_j} = A + BT + CT^2 + DT^3 + ET^4 + FT^5 \left(\frac{ft^2}{sec^2\ {}^oR} \right) \tag{40}$$

The coefficients in equation (40) are given in Table I. The values of C_{p_j} for He and Ar are:

$$C_{p_{He}} = 3.1025 \times 10^4 \ \frac{ft^2}{sec^2\ {}^oR} \tag{41}$$

$$C_{p_{Ar}} = 3.11151 \times 10^3 \ \frac{ft^2}{sec^2 \ ^oR} \tag{42}$$

The static enthalpy of the mixture is given by

$$h = (1 - c_f)\, h_i + c_f\, h_f \tag{43}$$

Where

$$h_i = \int_o^T C_{p_i}\, dT \tag{44}$$

and

$$h_f = \int_o^T C_{p_f}\, dT \tag{45}$$

Substituting equations (40), (41) and (42) into (44) and (45) results in a polynomial of the form

$$h_j = AT + BT^2 + CT^3 + DT^4 + ET^5 + FT^6 \left(\frac{ft^2}{sec^2}\right) \tag{46}$$

for air and CO_2 (the coefficients for equation (46) are given in Table II) and for He and Ar gives

$$h_{He} = 3.1025 \times 10^4 T \ \frac{ft^2}{sec^2} \tag{47}$$

$$h_{Ar} = 3.1115 \times 10^3 T \ \frac{ft^2}{sec^2} \tag{48}$$

6.3.2 Transport Properties

The transport properties calculated in this section are viscosity, thermal conductivity and the binary diffusion coefficient. The development of the thermal diffusion coefficient can be found in reference (20).

The viscosity of the mixture is obtained from Wilke's formula (reference 21) applied to a binary gas mixture.

$$\mu = \frac{\mu_i}{1 + G_{if} \frac{X_f}{X_i}} + \frac{\mu_f}{1 + G_{fi} \frac{X_i}{X_f}} \tag{49}$$

Where

$$X_i = \frac{(1 - c_f)/M_i}{c_f/M_f + (1 - c_f)/M_i} \tag{50}$$

$$X_f = \frac{c_f/M_f}{c_f/M_f + (1 - c_f)/M_i} \tag{51}$$

$$G_{if} = \frac{1}{\sqrt{8}} \left(1 + \frac{M_i}{M_f}\right)^{-1/2} \left[1 + \left(\frac{\mu_i}{\mu_f}\right)^{1/2} \left(\frac{M_f}{M_i}\right)^{1/4}\right]^2 \tag{52}$$

and μ_i, μ_f are viscosities of the individual species

The viscosities of the individual species are given by the Chapman-Enskog relation (reference 22).

$$\mu_j = 0.625 \frac{kT}{\Omega_j^{(2,2)}} \tag{53}$$

For temperatures less than 1000°K, the collision integral $\Omega_j^{(2,2)}$ is obtained from the Lennard-Jones (6-12) potential as tabulated in reference (22); Sutherland's law, reference (23), is used for air up to a temperature of 1500°K. For temperatures greater than 1000°K, the viscosities of He and Ar are obtained from Amdur and Mason (reference 24); where the collision integral was evaluated based upon an exponential repulsive potential of the form

$$\phi = Ae^{-r/\rho} \tag{54}$$

The viscosity of CO_2 for temperatures greater than 1000°K is taken from reference (25), where a Morse potential of the form

$$\phi = A\left[1 - e^{-B(r-c)}\right]^2 \tag{55}$$

is used to evaluate the collision integral. The viscosity of air for temperatures greater than 1500°K is calculated by using the mixture formula (equation (49)), and taking the composition of air to be essentially N_2 and O_2. The viscosity of N_2 is taken from Amdur and Mason, and the viscosity of O_2 is taken from reference (26). The viscosity data for all the gases have been fit to polynomials of the form

$$\mu_j = A + BT + CT^2 + DT^3 + ET^4 + FT^5 \left(\frac{\text{lb sec}}{\text{ft}^2}\right) \tag{56}$$

The coefficients in equation (56) are given in Table III.

The thermal conductivities of the individual species are given by the Eucken relation (reference 27)

$$\lambda_j = \frac{1}{4}\left(9\frac{C_{p_j}}{C_{V_j}} - 5\right) C_{V_j} \mu_j \tag{57}$$

The above relation takes molecular vibration and rotation into account in addition to the translation contribution to the internal energy. The thermal conductivity of the mixture is obtained by using equation (49) and replacing the individual species viscosities with the conductivities.

The binary diffusion coefficients are calculated from the first Chapman Enskog approximation (reference 22)

$$D_{fi} = 3k^2T^2/16pM_{fi}\Omega_{fi}^{(1,\ 1)} \tag{58}$$

where M_{fi} is the reduced mass of particles f, i.

The calculation of $D_{air\ i}$ is made by applying a reduced mass correction factor to calculated values of $D_{N_2\ i}$ (reference 28)

$$D_{air\ i} = D_{N_2\ i}\left(\frac{M_{N_2\ i}}{M_{air\ i}}\right)^{1/2} \tag{59}$$

For He, Ar and N_2, the collision integral $\Omega_{fi}^{(1,\ 1)}$ in equation (58) has been evaluated by Monchick (reference 29) on the basis of an exponential repulsive potential (equation (54)), where A and ρ are (reference 24).

	A (ev)	ρ (A^o)
He - He	0.0386×10^4	0.220
Ar - Ar	3.23×10^4	0.224
N_2 - N_2	1.35×10^4	0.263

To obtain the necessary combinations of these, a simple geometric mean combination rule (reference 24) is used

$$A_{fi} = \left(A_{ff}\,A_{ii}\right)^{1/2} \tag{60}$$

$$\frac{1}{\rho_{fi}} = \frac{1}{2}\left(\frac{1}{\rho_{ff}} + \frac{1}{\rho_{ii}}\right) \tag{61}$$

Using Monchick's results and equation (58) values of pD_{fi} were calculated and fitted to a fifth degree polynomial whose coefficients are given in Table IV.

For CO_2 the collision integral was calculated based upon the Lennard-Jones (6-12) potential (reference 22) up to a temperature of 1000°K. For temperatures greater than 1000°K, D_{fi} was calculated based upon the Sutherland model (reference 22)

$$D_{fi} = \frac{D(T)_{fi\text{ - rigid sphere}}}{1 + \frac{\theta}{T}} \tag{62}$$

where $D(T)_{fi\text{ - rigid sphere}}$ and θ are calculated from two known temperatures. pD_{fi} was calculated and fit to equation (62). The coefficients are given in Table IV.

It is stressed that the basic method of solution is the same for all three mixtures considered; the only differences appearing in the computer program are the numerical constants, appearing in the previous equations, used to describe properties of the individual species.

TABLE I

SPECIFIC HEAT AT CONSTANT PRESSURE

$$C_{P_j} = A + BT + CT^2 + DT^3 + ET^4 + FT^5 \left(\frac{ft^2}{sec^2\ {}^oR}\right)$$

Gas	Temperature Range ^oR	A	B	C	D	E	F
Air	$0 \le T \le 2000$	6.0351797×10^{3}	$-9.4509125 \times 10^{-4}$	$-7.3022675 \times 10^{-4}$	1.7322782×10^{-6}	$-9.7657438 \times 10^{-10}$	$1.7465179 \times 10^{-13}$
	$2000 \le T \le 6300$	6.4371993×10^{3}	$-4.4825613 \times 10^{-1}$	7.1435785×10^{-4}	$-2.4394435 \times 10^{-7}$	$3.4477526 \times 10^{-11}$	$-1.7810174 \times 10^{-15}$
CO_2	$0 \le T \le 2000$	2.3317627×10^{2}	7.3287082×10^{1}	-1.342833×10^{-1}	1.3090637×10^{-4}	$-6.0572879 \times 10^{-8}$	$1.0531063 \times 10^{-11}$
	$2000 \le T \le 6300$	1.328997×10^{4}	1.0499195×10^{1}	$-3.4760828 \times 10^{-3}$	6.1489558×10^{-7}	$-5.568993 \times 10^{-11}$	2.033227×10^{-15}

TABLE II

STATIC ENTHALPY

$$h_j = AT + BT^2 + CT^3 + DT^4 + ET^5 + FT^6 \left(\frac{ft^2}{sec^2}\right)$$

Gas	Temperature Range ^{o}R	A	B	C	D	E	F
Air	$0 \leq T \leq 2000$	6.0351797×10^{3}	$-4.7254562 \times 10^{-4}$	$-2.4340867 \times 10^{-4}$	4.3306955×10^{-7}	$-1.9531487 \times 10^{-10}$	$2.9108631 \times 10^{-14}$
	$2000 \leq T \leq 6300$	6.4371993×10^{3}	$-2.2412806 \times 10^{-1}$	2.3811928×10^{-4}	-6.098608×10^{-8}	6.895505×10^{-12}	$-2.968362 \times 10^{-16}$
CO_2	$0 \leq T \leq 2000$	2.3317627×10^{2}	$3.6643541 \times 10^{+1}$	-4.476109×10^{-2}	3.272659×10^{-5}	$-1.2114575 \times 10^{-8}$	1.755177×10^{-12}
	$2000 \leq T \leq 6300$	1.328997×10^{4}	5.249597	-1.158694×10^{-3}	1.5372389×10^{-7}	$-1.1137986 \times 10^{-11}$	3.388711×10^{-16}

TABLE III

VISCOSITIES

$$\mu_j \times 10^7 = A + BT + CT^2 + DT^3 + ET^4 + FT^5 \left(\frac{lb\ sec}{ft^2}\right)$$

$$90^\circ R \leq T \leq 6300\ ^\circ R$$

Gas	A	B	C	D	E	F
H_e	5.5026909 $\times 10^{-1}$	7.9471713 $\times 10^{-3}$	-2.2178108 $\times 10^{-6}$	4.0447782 $\times 10^{-10}$	-1.806356 $\times 10^{-14}$	-1.0112767 $\times 10^{-18}$
A_r	-5.5369992 $\times 10^{-2}$	1.0747731 $\times 10^{-2}$	-4.4382035 $\times 10^{-6}$	1.395966 $\times 10^{-9}$	-2.0667733 $\times 10^{-13}$	1.1450887 $\times 10^{-17}$
CO_2	-7.8193191 $\times 10^{-2}$	6.7732592 $\times 10^{-3}$	-17286911 $\times 10^{-6}$	3.8700139 $\times 10^{-10}$	-5.1304856 $\times 10^{-14}$	2.7591624 $\times 10^{-18}$
Air	-1.9336805 $\times 10^{-2}$	8.9325935 $\times 10^{-3}$	-3.918504 $\times 10^{-6}$	1.1728501 $\times 10^{-9}$	-1.649344 $\times 10^{-13}$	8.751547 $\times 10^{-18}$

TABLE IV

BINARY DIFFUSION COEFFICIENT

$$pD_{fi} = A + BT + CT^2 + DT^3 + ET^4 + FT^5 \left(\frac{lb}{sec}\right)$$

$$90^{\circ}R \leq T \leq 6300\ ^{\circ}R$$

Gas	A	B	C	D	E	F
H_e	$-9.7598318 \times 10^{-2}$	1.4399797×10^{-3}	3.9911825×10^{-6}	$-4.0516911 \times 10^{-10}$	$4.7053885 \times 10^{-14}$	$-2.3594221 \times 10^{-18}$
A_r	$-3.2467965 \times 10^{-2}$	4.8860752×10^{-4}	1.1704382×10^{-6}	$-1.3105574 \times 10^{-10}$	$1.4735018 \times 10^{-14}$	$-7.0980313 \times 10^{-19}$
CO_2	1.3094896×10^{-2}	$-5.6215733 \times 10^{-5}$	1.4178492×10^{-6}	$-3.8555763 \times 10^{-10}$	$6.8405177 \times 10^{-14}$	$-4.7403394 \times 10^{-18}$

6.4 Overall Method of Solution

The method used to solve equations (22) - (24) is based upon ideas originated by Hartree and Womersley (reference 12). This method has been applied to the incompressible laminar boundary-layer equations (reference 13), the compressible laminar boundary-layer equations (reference 14), and the laminar boundary-layer equations of a binary dissociating gas (reference 15). Many of the details of the method can be found in the aforementioned references. The essential differences between the work reported here and that reported in reference (15) is in the mathematical transformations and the fluid properties used. In addition a modification of the integration techniques used on the momentum and energy equations is introduced. The derivatives in the transformed streamwise direction appearing on the right-hand side of equations (22) - (24) are replaced by forward finite difference expressions. Thus at any given location along the surface the partial differential equations are approximated by ordinary differential equations provided solutions are known at upstream locations. Equations (22) - (24) are rewritten at station n along the body to give the following (it is to be understood that unless otherwise specified quantities are evaluated at station n, values at previous stations are denoted by subscripts):

Momentum

$$\left[C\,(1+t)\,\phi''\right]' = \beta\left(\phi_s^{\prime 2} + 2\phi' + 1 - \frac{\rho_e}{\rho}\right) - (\phi+\eta)\,\phi'' + R_1 \qquad (63)$$

Energy

$$\pi' = -\,(\phi+\eta)\,\psi' + R_2 \qquad (64)$$

Species

$$\Omega' = S(\phi'+1)\, z - (\phi+\eta)\, z' + R_3 \tag{65}$$

where

$$\phi' = f' - 1 \tag{66}$$

$$\psi = g - 1 \tag{67}$$

and

$$\pi = C(1+t)\left\{\frac{\psi'}{Pr} + \frac{u_e^2}{H_e}\left(1 - \frac{1}{Pr}\right)(\phi'+1)\phi'' + \frac{h_f - h_i}{H_e}\left[\frac{Le - 1}{Pr}\, c_{f_e}\, z' + \frac{D_f^T}{\mu}\,\frac{T'}{T}\right]\right\} \tag{68}$$

$$\Omega = C(1+t)\left(\frac{Le}{Pr}\, z' + \frac{D_f^T}{c_{f_e}\mu}\,\frac{T'}{T}\right) \tag{69}$$

The quantities ϕ' and ψ are introduced to reduce round off errors in the numerical integration of equations (63) and (64). These values go to zero at the edge of the boundary layer whereas the original dependent variables f' and g go to unity. The terms on the left-hand side of equations (63) - (65) contain the molecular transport quantities and are composed of the highest order derivatives in the direction normal to the surface. The quantities R_1, R_2, and R_3 contain the streamwise derivatives which are first order and are expressed in finite difference form, for example

$$R_1 = 2\bar{\xi}\left\{(\phi'+1)\left[a(\phi'+1) + b(\phi'_{n-1}+1) + c(\phi'_{n-2}+1)\right] - \phi''\left[a(\phi+\eta) + b(\phi_{n-1}+\eta) + c(\phi_{n-2}+\eta)\right]\right\} \tag{70}$$

Similar finite difference expressions are employed for R_2 and R_3. The quantities a, b, and c depend on the choice of step size for the independent variable $\bar{\xi}$; for the special case of equally spaced steps of length $\Delta\bar{\xi}$

$$a = 1.5/\Delta\bar{\xi} \qquad b = -2.0/\Delta\bar{\xi} \qquad c = 0.5/\Delta\bar{\xi}$$

if solutions are known at stations n-1 and n-2 equations (63), (64), and (65) are ordinary in ϕ, ψ, and z respectively. At station one, the three point finite difference expressions are replaced by two point finite difference expressions. No difficulty is encountered in starting at station zero since R_1, R_2, and R_3 are all zero at $\bar{\xi} = 0$.

Equations (63) - (65) are coupled and must be solved simultaneously. An iteration process is used (reference 15). At any given station n the initial fluid properties used are those obtained from the final solution at station n-1. The initial fluid properties are then used to obtain a solution to the momentum equation; the same fluid properties and stream function obtained from the solution of the momentum equation are used to solve the species and energy equations. Since the fluid properties and stream function are specified for any given solution of the species and energy equations, these equations are linear in z and ψ, respectively. The solutions to the species and energy equations are used to generate new fluid properties which are in turn used to obtain new solutions of the species and energy equations. This process is continued until the values of fluid properties converge. The same stream function is used for all cycles of this iteration loop. Upon convergence of fluid properties a new stream function is calculated using the latest fluid properties. This double iteration is continued until convergence of solutions to the momentum equation is obtained. The initial fluid properties used at

station zero are obtained by assuming a linear variation between the surface and edge conditions which are known boundary conditions.

6.4.1 Solution of the Momentum Equation

Equation (63) is a two point boundary value problem with two conditions at $\eta = 0$ and one condition at η_∞. That is

$$\phi(0) = \phi_w \text{ (specified)}$$

$$\phi'(0) = -1$$

$$\phi'(\eta_\infty) = 0$$

The boundary value problem is transformed to an initial value problem by hunting for the third condition at $\eta = 0$, namely $\phi''(0)$ which will give a solution satisfying the condition $\phi'(\eta_\infty) = 0$. With three conditions specified, $\phi(0)$, $\phi'(0)$, and $\phi''(0)$, equation (63) can be integrated. The right-hand side, RHS, of equation (63) is first integrated and ϕ'' is obtained from

$$\phi'' = \frac{1}{C(1+t)} \int_0^\eta \text{RHS}\ d\eta + \phi''(0) \qquad (71)$$

Successive integrations of ϕ'' then yield ϕ' and ϕ. It should be kept in mind that $C(1+t)$ is known from fluid properties which were obtained previously. Trial values of $\phi''(0)$ are used until three solutions have been bracketed within the bound $\pm K_1$ at η_∞. Once three solutions have been obtained and at least one solution is either high or low satisfying the condition

$$-K_1 \leq \phi'(\eta_\infty) \leq K_1$$

three point Lagrangian interpolation is used to obtain the final solution satisfying $\phi'(\eta_\infty) = 0$. A high solution is one in which $\phi'(\eta_\infty) > 0$ and a low solution is one in which $\phi'(\eta_\infty) < 0$. A predictor - corrector technique (pp 116-131, reference 30) is used to perform the integration indicated in equation (71). Solutions are started at the wall by means of a Taylor Series expansion and a shorter step size to maintain accuracy. See references (14) and (20) for details of the integration and the Lagrangian interpolation processes.

Under certain conditions it has been found that values of $\phi'(\eta_\infty)$ are extremely sensitive to trial values of $\phi''(0)$ and difficulty is encountered in bracketing three solutions at η_∞. In previous work (references 14 and 15) the original value input for η_∞ has been reduced when three solutions could not be bracketed. However in addition to the explicit boundary condition

$$\phi'(\eta_\infty) = 0$$

there exists the implicit condition that $\phi'' \longrightarrow 0$ as $\eta \longrightarrow \eta_\infty$.

Although the solution is forced to satisfy the explicit condition the implicit condition is satisfied only if η_∞ is sufficiently large. Hence, η_∞ can not be indiscriminately reduced in order to bracket three solutions. A method has been devised to overcome this difficulty. The essential feature of this method is that once $\phi''(0)$ has been determined to within a specified accuracy, the searching process for ϕ'' no longer continues at $\eta = 0$ but rather at some new value of η. Solutions are generated by incrementing or decrementing $\phi''(0)$, depending upon whether $\phi'(\eta_\infty)$ is low or high, a fixed amount until at least one high and one low solution is obtained. From then on trial values of $\phi''(0)$ are obtained by bisection.

If three solutions have not been bracketed within bound $\pm K_1$ and for two successive trial values $\phi_i''(0)$ and $\phi_{i+1}''(0)$ the following condition exists

$$\frac{\left|\phi_{i+1}''(0) - \phi_i''(0)\right|}{\phi_{i+1}''(0) + \phi_{i+1}''(0)} < \epsilon_1$$

then integration is begun at η_{s1} where η_{s1} is the maximum value of η at which the last high and low ϕ' profiles differ by a small amount, ϵ_2. The trial velocity profiles ϕ' agree at $\eta = 0$ and the difference between them grows with η; hence, it can be said that the velocity profile has been determined to within ϵ_2 up to η_{s1}. The last three profiles, of which at least one is either high or low, are now used as the basis for beginning the search at η_{s1}. Let the subscripts 1, 2, 3 refer to these last three profiles where 1 refers to the low profile, 2 to the middle profile, and 3 the high profile. The quantities $\phi_2(\eta_{s1})$ and $\phi_2'(\eta_{s1})$ are used as initial values for succeeding integrations from η_{s1}. Trial values of $\phi''(\eta_{s1})$ are now used to obtain new solutions. The first new solution is obtained by subtracting from or adding to $\phi_2''(\eta_{s1})$, depending upon whether $\phi_2'(\eta_\infty)$ is high (>0) or low (<0), one fourth the difference between $\phi_1''(\eta_{s1})$ and $\phi_3''(\eta_{s1})$. The process of adding or subtracting one fourth the difference between the last high and low solutions to the last trial value of $\phi''(\eta_{s1})$ is continued until a high and low solution are obtained; then bisection between the high and low is continued until three values of $\phi'(\eta_\infty)$ have been bracketed or

$$\frac{\left|\phi_{i+1}''(\eta_{s1}) - \phi_i''(\eta_{s1})\right|}{\phi_{i+1}''(\eta_{s1}) + \phi_i''(\eta_{s1})} < \epsilon_1$$

If the latter condition is met and three solutions are still not bracketed, integration begins at η_{s2} with trial values of $\phi''(\eta_{s2})$ where η_{s2} is now the maximum value at which the last high and low solutions differ by ϵ_2. This procedure is continued J times; that is until trial solutions have been attempted from η_{sJ}. The quantities ϵ_1, ϵ_2 and J are inputs to the program; typical values are 10^{-8}, 10^{-6}, and 4 respectively.

The process of extending the trajectory of integration (ETI) by beginning from a new location has also been applied to the species and energy equations and a schematic diagram of the process applicable to the energy equation is shown in Figure 2.

6.4.2 Solution of the Species Equation

With values of the stream function and fluid properties known, it can be seen that equation (65) is linear in z. The usual specified boundary condition at the wall will be z(0). The equation is second order and a value of z'(0) in addition to z(0) will provide the necessary information to be able to treat the solution as an initial value problem. Two trial values $z_1'(0)$ and $z_2'(0)$ are used to obtain z_1 and z_2. These solutions are combined linearly to give a general solution

$$z = Az_1 + Bz_2 \tag{72}$$

and then the coefficients A and B are obtained from the two boundary conditions

$$z(0) = z_w \text{ (specified)} \quad \text{and} \quad z(\eta_\infty) = 1$$

to give a particular solution.

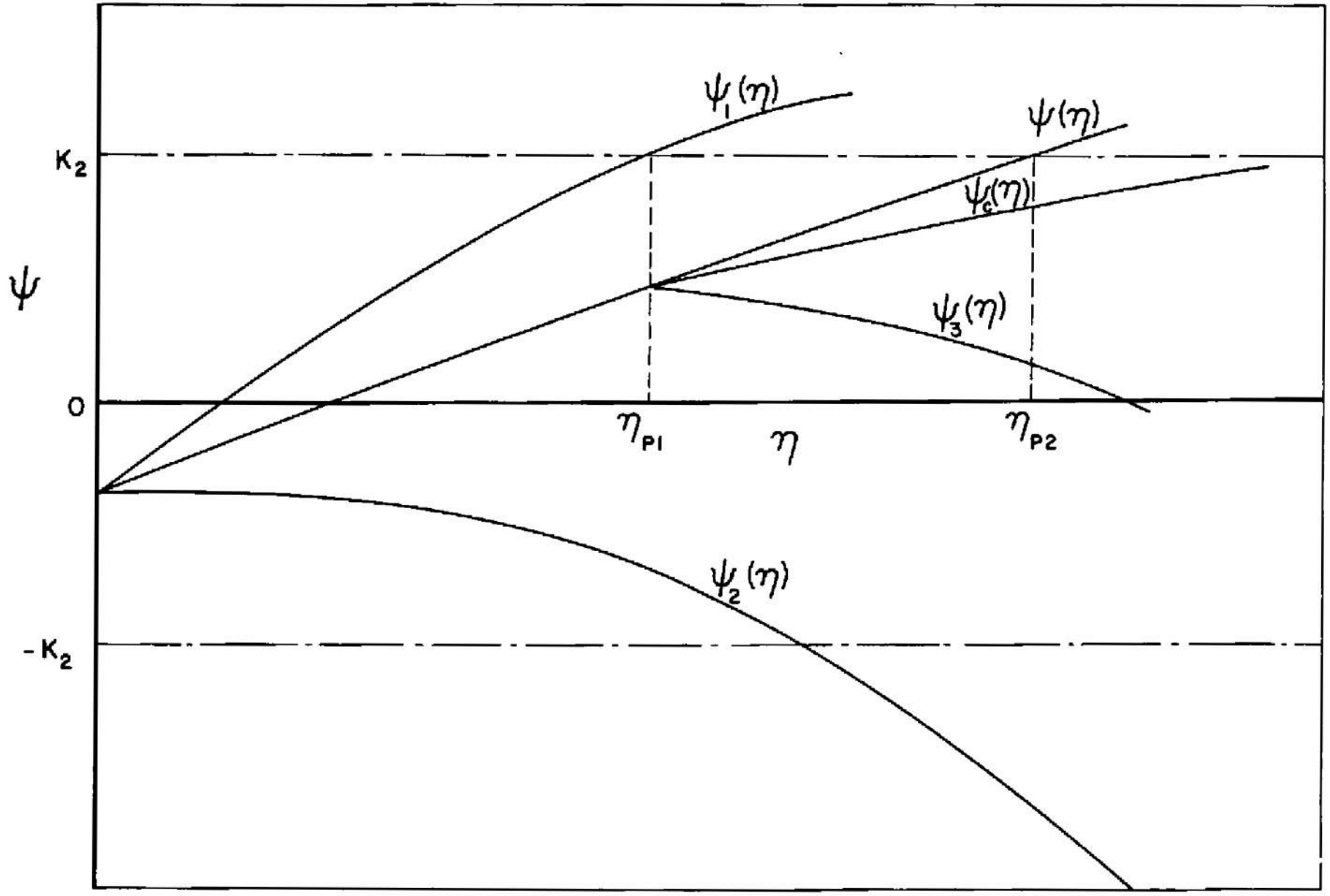

Figure 2. - Diagram of Solution to Energy Equation

AEDC-TR-66-183

The quantity z'(0) may be specified as a boundary condition instead of z(0). In this case, two trial values of z(0) are used to obtain two solutions which are combined to give a general solution. The particular solution is then obtained by satisfying the boundary conditions

$$z'(0) = z'_w \text{ (specified)} \quad \text{and} \quad z(\eta_\infty) = 1$$

The coefficients A and B in equation (72) obtained from the boundary conditions are

$$A = \frac{1 - z_2(\eta_\infty)}{z_1(\eta_\infty) - z_2(\eta_\infty)} \tag{73}$$

$$B = 1 - A \tag{74}$$

As with the momentum equation, the quantity R_3 is replaced by a finite difference expression and equation (65) becomes ordinary and is integrated in the η direction at successive values of $\bar{\xi}$. The solution at any value of $\bar{\xi}$ utilizes solutions at the two previous values of $\bar{\xi}$.

Once z(0) and z'(0) are specified a solution z is obtained by using the specified initial conditions and integrating the right-hand side of equation (65) to give Ω. Once Ω is determined, z' is obtained from equation (69) and z is obtained by integration of z'. The same integration formulas (pp. 116 - 131, reference 30) used on the momentum equation are used to perform the necessary integrations to obtain a solution to the species equation.

6.4.3 Solution to the Energy Equation

Equation (64) is linear in ψ since fluid properties and the stream function are known from a previous solution. The same general procedure

used to solve the species equation is used on the energy equation. The quantity R_2 is expressed in finite difference form to make the equation ordinary. The specified surface boundary condition may be either $\psi(0)$ or $\psi'(0)$. If $\psi(0)$ is specified two trial values $\psi_1'(0)$ and $\psi_2'(0)$ are used to produce solutions ψ_1 and ψ_2; these solutions are linearly combined to give a general solution and then the boundary conditions

$$\psi(0) = \psi_w \text{ (specified)}$$

and

$$\psi(\eta_\infty) = 0$$

are satisfied to obtain the particular solution.

The general solution is given by

$$\psi = A\psi_1 + B\psi_2 \tag{75}$$

where the coefficients obtained from satisfying boundary conditions are given by

$$A = \frac{-\psi_2(\eta_\infty)}{\psi_1(\eta_\infty) - \psi_2(\eta_\infty)} \tag{76}$$

$$B = 1 - A \tag{77}$$

With given initial conditions $\psi(0)$ and $\psi_1'(0)$, the right-hand side of equation (64) is integrated to give π. Equation (68) is solved for ψ_1' which is then integrated to give ψ_1 and a similar procedure is used to obtain ψ_2.

If the two trial solutions ψ_1 and ψ_2 are highly divergent, the linearization technique over the complete range from zero to η_∞ can break down. In this case, a modified procedure is used to obtain a solution. A set of coefficients A_o and B_o are computed as before using equations (76) and (77); however, it is assumed that the final solution is valid only out to η_{Pl} where η_{Pl} is the minimum value at which either ψ_1 or ψ_2 exceeds the bound K_2. (See Figure 2.)

That is

$$\psi = A_o \psi_1 + B_o \psi_2 \quad \text{for } o \leq \eta \leq \eta_{Pl} \tag{78}$$

a new solution ψ_3 is now generated from η_{Pl} using $\psi(\eta_{Pl})$ and $\psi_t'(\eta_{Pl})$ as initial conditions where

$$\psi(\eta_{Pl}) = A_o \psi_1(\eta_{Pl}) + B_o \psi_2(\eta_{Pl}) \tag{79}$$

and $\psi_t'(\eta_{Pl})$ represents a small perturbation of $\psi'(\eta_{Pl})$. The new solution ψ_3 is now linearly combined with ψ to give a continuation ψ_c of the original solution

$$\psi_c = A_1 \psi + B_1 \psi_3 \text{ for } \eta_{Pl} \leq \eta \leq \eta_{P2} \tag{80}$$

The process is continued until a complete solution out to η_∞ has been obtained. The quantities K_2 and ϵ_3 are inputs to the program and are typically 100 and 10^{-3} respectively.

6.5 Boundary Layer Parameters

Once the profiles of ϕ, z, ψ and their derivatives have been determined at an x-station, the program determines the conventional boundary-layer parameters of displacement thickness, momentum thickness, local skin friction, and local heat transfer. The program calculates a set of these parameters for the Levy-Lees transformation designated as t equal to zero, and for the Levy-Lees Probstein-Elliott transformation including second-order transverse curvature, designated as t not equal to zero (for this case t is given by equation (25)).

If TVC is neglected the following expressions are used:

The displacement thickness is calculated from the formula

$$\delta^* = \int_0^\infty \left(1 - \frac{\rho u}{\rho_e u_e}\right) dy \tag{81}$$

when transformed to the ξ, η - coordinates equation (81) becomes

$$\delta^* = \frac{(2\xi)^{1/2}}{\rho_e u_e r_o^k} \int_0^\infty \left(\frac{\rho_e}{\rho} - f'\right) d\eta \tag{82}$$

The program calculates normalized displacement thickness Δ^*, which is defined by

$$\Delta^* = (Re_x)^{1/2} \frac{\delta^*}{r_o^k} = \frac{x}{r_o^{2k}\,\mu_e} \left(\frac{2\xi}{Re_x}\right)^{1/2} \left[\int_0^\infty \left(\frac{\rho_e}{\rho} - f'\right) d\eta\right] \tag{83}$$

where

$$Re_x = \frac{\rho_e u_e x}{\mu_e}$$

The program calculates y from η using the following relationship

$$\eta = \frac{\rho_e u_e}{(2\xi)^{1/2}} \int_0^y \frac{\rho}{\rho_e} r_o^k \, dy \tag{84}$$

or

$$y = \frac{(2\xi)^{1/2}}{r_o^k \rho_e u_e} \int_0^\eta \frac{\rho_e}{\rho} \, d\eta \tag{85}$$

A normalized y is defined

$$Y = (Re_x)^{1/2} \frac{y}{r_o^k} \tag{86}$$

and calculated from

$$Y = \frac{x}{r_o^{2k} \mu_e} \left(\frac{2\xi}{Re_x}\right)^{1/2} \int_0^\eta \frac{\rho_e}{\rho} \, d\eta \tag{87}$$

The momentum thickness is given by

$$\theta = \int_0^\infty \frac{\rho u}{\rho_e u_e} \left(1 - \frac{u}{u_e}\right) dy \tag{88}$$

or in ξ, η - coordinates by

$$\theta = \frac{(2\xi)^{1/2}}{\rho_e u_e r_o^k} \int_0^\infty f'(1-f') \, d\eta \tag{89}$$

A normalized momentum thickness is calculated from

$$\theta = (Re_x)^{1/2} \frac{\theta}{r_o^k} = \frac{x}{r_o^k \mu_e} \left(\frac{2\xi}{Re_x}\right)^{1/2} \left[\int_o^\infty f'(1-f') \, d\eta \right] \tag{90}$$

The shear stress at the wall is

$$\tau_w = \mu_w \left(\frac{\partial u}{\partial y}\right)_w \tag{91}$$

and in ξ, η coordinates

$$\tau_w = \frac{\rho_w \mu_w u_e^2 r_o^k f''_w}{(2\xi)^{1/2}} \tag{92}$$

Introducing the local skin friction coefficient defined as

$$c_f = \frac{\tau_w}{\frac{1}{2} \rho_e u_e^2} \tag{93}$$

gives

$$c_f = \left(\frac{2}{\xi}\right)^{1/2} \frac{\rho_w}{\rho_e} \mu_w r_o^k f''_w \tag{94}$$

The heat transfer at the wall is

$$-q_w = \left\{ \lambda \frac{\partial T}{\partial y} + (h_f - h_i) \left[\rho D_{fi} \frac{\partial c_f}{\partial y} + D_f^T \frac{1}{T} \frac{\partial T}{\partial y} \right] \right\}_w \tag{95}$$

$$-q_w = \left\{ \frac{\lambda}{\overline{C}_p} \frac{\partial h}{\partial y} + (h_f - h_i) \frac{\lambda}{\overline{C}_p} \left[(L_e - 1) \frac{\partial c_f}{\partial y} + \frac{\overline{C}_p}{\lambda} D_f^T \frac{1}{T} \frac{\partial T}{\partial y} \right] \right\}_w \quad (96)$$

In terms of ξ, η-coordinates

$$-q_w = \frac{\mu_w \rho_w u_e H_e r_o^k}{Pr_w (2\xi)^{1/2}} \left\{ g'_w + \left(\frac{h_f - h_i}{H_e} \right)_w \right.$$

$$\left. \left[(Le - 1) c_{f_e} z' + \frac{Pr D_f^T}{T\mu} T' \right]_w \right\} \quad (97)$$

The Stanton number is defined as

$$St = \frac{-q_w}{\rho_e u_e H_e (1-g_w)} \quad (98)$$

$$St = \frac{\mu_w \rho_w r_o^k}{Pr_w \rho_e (1-g_w) (2\xi)^{1/2}} \left\{ g_w' \right.$$

$$\left. + \left(\frac{h_f - h_i}{H_e} \right)_w \left[(Le-1) c_{f_e} z' + \frac{Pr D_f^T}{\mu T} T' \right]_w \right\} \quad (99)$$

If TVC is included the following expressions are used:

The displacement thickness is given by

$$\delta^* \left(1 + \frac{\delta^*}{2r_o} \cos\alpha\right) = \int_o^\infty \left(\left(1 - \frac{\rho u}{\rho_e u_e}\right)\left(1 + \frac{y}{r_o} \cos\alpha\right) dy \right. \tag{100}$$

To express δ^* in $\bar{\xi}$, $\bar{\eta}$ coordinates

$$d\bar{y} = \left(\frac{r_o}{L} + \frac{y}{L} \cos\alpha\right) dy \tag{101}$$

and

$$\delta^* = \frac{r_o}{\cos\alpha}\left[-1 + \left(1 + \frac{2L\cos\alpha}{r_o^2 \rho_e u_e}(2\bar{\xi})^{1/2} \int_o^\infty \left(\frac{\rho_e}{\rho} - f'\right) d\bar{\eta}\right)^{1/2}\right] \tag{102}$$

A normalized displacement thickness is defined by

$$\Delta^* = (Re_x)^{1/2} \frac{\delta^*}{r_o} \tag{103}$$

and calculated from

$$\Delta^* = \frac{(Re_x)^{1/2}}{\cos\alpha}\left[-1 + \left(1 + A \int_o^\infty \left(\frac{\rho_e}{\rho} - f'\right) d\bar{\eta}\right)^{1/2}\right] \tag{104}$$

where

$$A = \frac{2L\cos\alpha}{r_o^2 \rho_e u_e}(2\bar{\xi})^{1/2} \tag{105}$$

The transformation to $\bar{\eta}$ and its inverse are:

$$\bar{\eta} = \frac{\rho_e u_e}{(2\bar{\xi})^{1/2}} \int_0^{\bar{y}} \frac{\rho}{\rho_e} \, d\bar{y} \tag{106}$$

$$\bar{y} = \frac{(2\bar{\xi})^{1/2}}{\rho_e u_e} \int_0^{\bar{\eta}} \frac{\rho_e}{\rho} \, d\bar{\eta} \tag{107}$$

using equation (101)

$$y = \frac{r_o}{\cos\alpha} \left[-1 + \left(1 + \frac{2L\cos\alpha}{r_o^2 \rho_e u_e} (2\bar{\xi})^{1/2} \int_0^{\bar{\eta}} \frac{\rho_e}{\rho} \, d\bar{\eta} \right)^{1/2} \right] \tag{108}$$

a normalized y is defined below

$$Y = (Re_x)^{1/2} \frac{y}{r_o}$$

and calculated from

$$Y = \frac{(Re_x)^{1/2}}{\cos\alpha} \left[-1 + \left(1 + A \int_0^{\bar{\eta}} \frac{\rho_e}{\rho} \, d\bar{\eta} \right)^{1/2} \right] \tag{109}$$

where A is defined by equation (105)

The momentum thickness is given by

$$\theta \left(1 + \frac{\theta}{2r_o} \cos\alpha \right) = \int_0^{\infty} \frac{\rho u}{\rho_e u_e} \left(1 - \frac{u}{u_e} \right) \left(1 + \frac{y}{r_o} \cos\alpha \right) dy \tag{110}$$

and in $\bar{\xi}$, $\bar{\eta}$ coordinates becomes

$$\theta = \frac{r_o}{\cos\alpha}\left[-1 + \left(1 + A\int_o^\infty f'\,(1-f')\,d\eta\right)^{1/2}\right] \tag{111}$$

A normalized momentum thickness is defined by

$$\theta = (Re_x)^{1/2}\,\frac{\theta}{r_o} \tag{112}$$

and obtained from

$$\theta = \frac{(Re_x)^{1/2}}{\cos\alpha}\left[-1 + \left(1+A\int_o^\infty f'\,(1-f')\,d\bar{\eta}\right)^{1/2}\right] \tag{113}$$

The shear stress obtained from equation (91)

in $\bar{\xi}$, $\bar{\eta}$ coordinates is given by

$$\tau_w = \frac{\rho_w \mu_w u_e^2 r_o f''_w}{L\,(2\bar{\xi})^{1/2}} \tag{114}$$

Introducing c_f defined by equation (93) gives

$$c_f = \left(\frac{2}{\bar{\xi}}\right)^{1/2}\frac{r_o}{L}\,\frac{\rho_w}{\rho_e}\,\mu_w\,f''_w \tag{115}$$

The surface heat transfer obtained from equation (95) in

$\bar{\xi}$, $\bar{\eta}$ coordinates is given by

$$-q_w = \frac{\mu_w \rho_w u_e H_e r_o}{L Pr_w (2\bar{\xi})^{1/2}} \left\{ g'_w + \left(\frac{h_f - h_i}{H_e} \right)_w \right.$$

$$\left. + \left[(Le-1) c_{f_e} z' + \frac{Pr D_f^T}{\mu T} T' \right]_w \right\} \qquad (116)$$

Stanton number is given by equation (98) and becomes

$$St = \frac{\mu_w \rho_w r_o}{Pr_w L \rho_e (1-g_w) (2\bar{\xi})^{1/2}} \left\{ g'_w \right.$$

$$\left. + \left(\frac{h_f - h_i}{H_e} \right)_w \left[(Le-1) c_{f_e} z' + \frac{Pr D_f^T}{\mu T} T' \right]_w \right\} \qquad (117)$$

7.0 RESULTS AND DISCUSSION

The laminar boundary-layer flow field was calculated for a 9° half-angle cone at a free stream Mach number of 10 and free stream Reynolds number, based on cone slant length, of 940. Cases were computed with and without mass injection. The following edge conditions were used for all cases computed:*

$u_e = 7897.0$ ft/sec $\qquad \rho_e = 3.485 \times 10^{-7}$ lb sec^2/ft^4

$H_e = 3.395 \times 10^7$ ft^2/sec^2 $\qquad T_e = 460.09$ °R

$p_e = 0.2749$ lb/ft^2 $\qquad \mu_e = 3.368 \times 10^{-7}$ lb sec/ft^2

$c_{f_e} = 1.0$

The conditions at the wall are specified by f_w, g_w, and z_w. At locations where the wall is solid f_w is zero; at locations where mass injection takes place f_w is given by equation (30a). If TVC (transverse curvature) is neglected f_w is given by a slightly modified form of equation (30a), shown below

$$f_w = -\frac{1}{(2\xi)^{1/2}} \int_0^x \rho_w v_w r_o \, dx$$

* These values are within the range of test conditions of the AEDC-VKF Low Density Tunnel L.

It should be kept in mind that without TVC the Probstein-Elliott transformation is not used and the independent variables are unbarred. The value of g_w used is based on a surface temperature of 1116.6°R; for pure air this corresponds to a value for g_w of 0.2. The value of z_w is unity at surface locations with no mass transfer and is zero at locations where there is injection of a foreign gas.

The body used for computational purposes is based on a test model employed at AEDC-VKF. It is a 9° half-angle cone with solid front section followed by a porous section used for mass injection. Taking the slant length of the cone as ℓ the porous section begins at an x/ℓ of 0.4218. The actual length of the test model is 2.397 in. and the free stream Reynolds number used is based on this length. In all cases calculated with blowing the mass injection rate is assumed uniform from 0.4218ℓ to the base of the cone (see Figure 3).

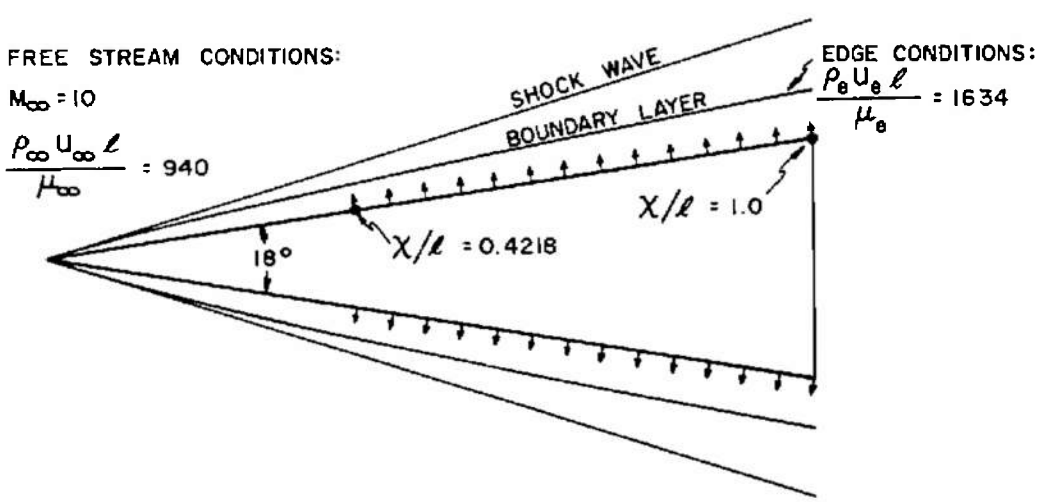

Figure 3. - Diagram of Cone Model

The results presented in this section are for calculations both with and without the TVC term included in the equations. Both sets of results are exhibited in order to provide a basis for comparison of predicted values obtained from a standard Mangler treatment with values obtained from an exact treatment of TVC.

The TVC term t as can be seen from equation (25) is of the form

$$t = F(\bar{\xi}) \int_0^{\bar{\eta}} \frac{\rho_e}{\rho} \, d\bar{\eta}$$

where the function $F(\bar{\xi})$ is well behaved if the radius of the body is finite. However, if the radius is zero, which is the case at the tip of a cone, $F(\bar{\xi})$ becomes singular. Trial solutions indicated that downstream solutions are insensitive to the value of F(0). Numerical solutions were obtained first by neglecting F(0) and using various distributions of $\bar{\xi}$ near the tip of the cone. The different solutions converged to the same values downstream of the tip and it was shown that the region of convergence moved upstream as locations closer to the tip were used. Neglecting F(0), however, did cause the results in a region near the tip to be of questionable accuracy; for example, the skin friction coefficient rather than decreasing monotonically exhibited a slight dip and rise near the tip prior to decreasing. This phenomenon was eliminated by employing a value of F(0) which is higher than $F(\bar{\xi}_1)$ where $\bar{\xi}_1$ is the first location past the tip at which a solution is obtained. In all calculations involving TVC, the first station past the tip was taken at a value of $\bar{\xi}$ of 0.236231×10^{-22}; this corresponds to an x/ℓ of 2.5×10^{-4}. As the solution proceeded downstream, larger increments of $\bar{\xi}$ could be handled and a total of 27 stations were used for the complete cone. The value of

$F(0.236231 \times 10^{-22})$ for the particular flow studied here is 16.1496 and F(0) was arbitrarily chosen as 32. An examination of equations (22), (23) and (24) indicates that as larger values of F(0) are used the values of $f''(0)$, $g'(0)$, and $z'(0)$ increase and in the limit as $F(0) \longrightarrow \infty$ f', g, and z are unity for all η greater than zero. The use of a large value for F(0) will provide steep gradients at the wall and hence provide reasonable starting profiles.

The Hartree Womersley method was originally developed to handle a one component gas (references 14 and 31). A different transformation than is employed in the present investigation was used and the method was programmed for pure air. In the present investigation, if z is unity and z' is zero for the whole boundary layer, then the binary mixture equations reduce to those describing pure air. Although the solution of the species equation would yield a z of unity throughout the boundary layer for a single component, an option was incorporated in the computer program which can be used to bypass the solution of the species equation and automatically yield a value of unity for z and zero for z'. The fluid properties computed are then those of pure air. Using this option, the boundary layer with mass injection of air on the body, shown in Figure 3, was computed neglecting TVC and compared to results using the method described in references 14 and 31. The fluid property relations used in the two methods and the mathematical transformations differ; values of displacement thickness and Stanton number divided by skin friction coefficient shown in Table V are in fair agreement. This comparison was made primarily for the purpose of checking the system of reducing the binary mixture equations to those for a single component.

Figures 4 through 11 and Tables VI and VII exhibit results from calculations both neglecting and including TVC and employing helium, air, argon and carbon dioxide as the injected gas.

Since viscous interaction is neglected in the present calculations, the quantity β appearing in equation (22) is zero and since the free stream is pure air for all locations along the cone, the quantity S appearing in equation (24) is zero. The circled points in Figures 5(b) and 10(b) indicate locations on the cone at which solutions to equations (22) through (24) were obtained. Intervals of 0.05 of the transformed y coordinate were used with smaller step sizes (see references 20 and 31) near the wall to maintain accuracy.

Probstein and Elliott (reference 16) point out that the additional term in the differential equations arising from the inclusion of the transverse curvature effect causes behavior similar to that of a favorable pressure gradient. Examination of the figures and tables indicate that inclusion of the TVC term causes predictions of skin friction coefficient and Stanton number to be higher and predictions of displacement thickness lower than predictions based upon calculations which neglect TVC; hence, the present results agree with the aforementioned observation of Probstein and Elliott.

The computed results show that, in general, the effect of TVC increases with decreasing molecular weight; hence, its effect is greater for helium injection than injection of any of the other gases. This result is explained by the fact that the TVC term t appearing in the equations contains the quantity $\int \rho_e/\rho \, d\bar{\eta}$ which increases with decreasing molecular weight. Moreover, the results indicate that inclusion of TVC predicts values of the various boundary layer parameters which differ significantly from values obtained

from calculations which neglect the TVC effect. For example (see Figures 5(a) and 9(a)) with no mass injection, the skin friction coefficient at $x/\ell = 1.0$ is about 50% greater when TVC is included. It is also shown (see Tables VI and VII), that the relative effect of helium injection in comparison to air injection is far less pronounced when TVC is taken into account.

Of interest in connection with the results obtained here are experimental results reported by King and Talbot (reference 9) which show that for a given injection rate air has a greater effect on the drag coefficient than does helium. The present results in this respect do not agree with experiment; however, it can be said that the inclusion of TVC in the calculations greatly improves matters regarding agreement between theory and experiment.

It is felt that inclusion of the boundary layer displacement effect on the external flow would be one further refinement which might clear up the discrepancy between theory and experiment. This effect would introduce a favorable gradient and as with TVC the effect would increase with decreasing molecular weight since the pressure gradient term appearing in the momentum equation (i.e., see equation (22)) contains the quantity ρ_e/ρ.

The present results indicate the importance of solutions utilizing accurate fluid properties to ascertain the relative effects of various injection gases on the boundary layer. For example, a simplified treatment based solely on the molecular weight effect would predict a decreasing effect on c_f of mass injection with increasing molecular weight of the injected gas. This is due to the effect of the molecular weight on the quantity C. However, as can be seen from the results in Tables VI and VII, the present investigation indicates the opposite effect with regard to injection of argon, and carbon

dioxide. This result is due to the fact that the quantity C is temperature dependent and the heat capacity effect of the injected gas must be taken into account. The present investigation indicates that carbon dioxide injection has a greater effect on reduction of c_f than argon injection. Although the molecular weight of carbon dioxide is greater, the temperature distribution produced by its injection is considerably lower than that for argon injection (see Figures 8(b) and 11(b)) due to its high heat capacity; hence, the net effect on c_f is greater than that for argon injection. It is expected, however, that the heat capacity effect would decrease with decreasing surface temperatures and at low Mach numbers the effect of injection would be directly related to molecular weight.

In addition to the effect of including TVC on the skin friction predictions, interesting effects are produced regarding predictions of heat transfer. The results in Table VI based on calculations without TVC indicate that the Stanton number for helium injection is lower than that for any of the other gases. For a binary mixture, the surface heat transfer rate (see equation (95)) is composed of a temperature gradient term and concentration gradient term. Since the heat capacity of helium is much greater than that of air, the concentration gradient will contribute to a heat flux away from the wall and the temperature gradient term which contributes to a heat flux towards the surface will be lowered by the heat capacity effect. The net result indicates heat transfer away from the wall for the set of conditions investigated here. However, with TVC (see Table VII), the conduction term is increased to the point where the net result is heat transfer to the wall. Thus, without TVC, helium appears to be the best coolant of the gases studied here, and with TVC, carbon dioxide appears to be the best coolant. Again, this is due to the fact that the effects of

including transverse curvature are felt the most with helium injection and the least with carbon dioxide injection.

TABLE V

COMPARISON OF COMPUTED BOUNDARY LAYER PARAMETERS FOR AIR INJECTION NEGLECTING TVC - Pr = 0.71

$$\frac{\rho_w v_w}{\rho_e u_e} = 0.01434$$

x/ℓ	St $/c_f$		δ^*/ℓ	
	Present Method	Reference 31	Present Method	Reference 31
0.20	0.5071	0.5088	0.0570	0.0581
0.45	0.5383	0.5327	0.0956	0.0962
0.60	0.5410	0.5490	0.1200	0.1308
0.72	0.5509	0.5573	0.1397	0.1508
0.86	0.5627	0.5675	0.1628	0.1737
0.90	0.5758	0.5705	0.1694	0.1801
0.96	0.5708	0.5752	0.1785	0.1897
1.00	0.5740	0.5783	0.1846	0.1962

TABLE VI

COMPUTED BOUNDARY LAYER PARAMETERS, NEGLECTING TVC – VARIABLE FLUID PROPERTIES

$$\frac{\rho_w v_w}{\rho_e u_e} = 0.01147$$

INJECTED GAS	x/ℓ = 0.75			x/ℓ = 0.90		
	δ^*/ℓ	c_f	St x 10	δ^*/ℓ	c_f	St x 10
He	0.3183	0.0036	-0.1536	0.3695	0.0022	-0.2355
Air	0.1398	0.0140	0.0747	0.1595	0.0114	0.0616

$$\frac{\rho_w v_w}{\rho_e u_e} = 0.01434$$

Air	0.1459	0.0117	0.0636	0.1699	0.0089	0.0493
Ar	0.1452	0.0162	0.0972	0.1700	0.0126	0.0768
CO_2	0.1070	0.0159	0.0381	0.1240	0.0124	0.0308

TABLE VII

COMPUTED BOUNDARY LAYER PARAMETERS,
INCLUDING TVC – VARIABLE FLUID PROPERTIES

$$\frac{\rho_w v_w}{\rho_e u_e} = 0.01434$$

INJECTED GAS	$x/\ell = 0.75$			$x/\ell = 0.90$		
	δ^*/ℓ	c_f	St x 10	δ^*/ℓ	c_f	St x 10
He	0.1937	0.0147	0.6603	0.2475	0.0099	0.1656
Air	0.1266	0.0232	0.1205	0.1434	0.0191	0.1001
Ar	0.1280	0.0298	0.1723	0.1451	0.0249	0.1439
CO_2	0.1060	0.0245	0.0529	0.1185	0.0203	0.0491

8.0 CONCLUDING STATEMENTS

The method described in this report has proven capable of solving the binary diffusion laminar boundary layer equations. It is applicable to axisymmetric flows with or without transverse curvature effects included and to two-dimensional flows. The mathematical transformations used make it possible to easily include or neglect the transverse curvature terms within the framework of one computer program. A combination of the Probstein-Elliott and Levy-Lees transformations introduces a common term t to the system of equations being solved. If this term is retained, the higher order transverse curvature effects are accounted for in the numerical solution to the equations; if this term is neglected, the equations assume the standard Levy-Lees form and the second-order transverse curvature effects are not accounted for. The general method of solution is identical for both cases; however, the proper inverse transformations used to go back to the physical plane depend on whether or not the quantity t is included or neglected in the solution of the partial differential equations.

The method of solution has been programmed for the IBM 7094 computer for the following mixtures: helium-air, argon-air, and carbon dioxide-air. The program also contains an option which bypasses the solution of the species equation when a calculation with pure air is desired. Variable fluid properties given as functions of local temperature and mass fraction throughout the boundary layer are used. Although the equations appear to be more complex when second-order transverse curvature is accounted for, the actual computing times are less. This is due to the fact that convergence of trial solutions of the momentum equation is more rapid

when the transverse curvature term appears in the equation. Approximately 21 stations along the cone were used to obtain solutions neglecting the TVC term and 27 stations were used when it was included. The total computing times for the complete body were about 47 minutes and 36 minutes respectively.

The results indicate that the TVC effect is significant and increases with decreasing molecular weight. As a corollary of this, the effect of helium injection on the reduction of skin friction relative to the effect of air injection is far less pronounced when TVC is taken into account. Solutions to the equations containing the TVC term yield values of skin friction coefficient and Stanton number higher and values of displacement thickness lower than solutions which neglect this term.

The results obtained indicate the necessity of using exact fluid properties to ascertain the relative effects of injection of various gases.

The investigation of viscous interaction for hypersonic flow over slender cones with mass injection is recommended for future study. This investigation could be conducted by using the present method together with an iteration between external pressure distribution and computed displacement thickness. It is felt that the viscous interaction effect will increase with decreasing molecular weight of the injected gas and, in general, will cause behavior similar to that caused by inclusion of the transverse curvature effect.

9.0 REFERENCES

1. Baron, J. R.: The Binary Mixture Boundary Layer Associated with Mass Transfer Cooling at High Speeds. Massachusetts Institute of Technology, Naval Supersonic Laboratory, Technical Report No. 16, May 1956.

2. Covert, E. E.: Some Approximations to the Solution to the Binary Boundary - Layer Problem. Massachusetts Institute of Technology, Naval Supersonic Laboratory, Technical Report No. 390, September 1959.

3. Baron, J. R. and Scott, P. B.: The Laminar Diffusion Boundary Layer with External Flow Field Gradients. Massachusetts Institute of Technology, Naval Supersonic Laboratory, Technical Report No. 419, December 1959.

4. Moran, J. P. and Scott, P. B.: A Mass Transfer Finite Difference Formulation Employing Crocco Variables. Massachusetts Institute of Technology, Naval Supersonic Laboratory, Technical Report No. 443, June 1960.

5. Flügge-Lotz, I. and Baxter, D. C.: The Solution of Compressible Laminar Boundary Layer Problems by a Finite Difference Method, Part 1, Description of the Method. Stanford University, Division of Engineering Mechanics, Technical Report No. 103, October 1957.

6. Moran, J. P.: Application of Covert's Approximations for the Binary Boundary - Layer to a Porous Cone with a Solid Tip. Massachusetts Institute of Technology, Naval Supersonic Laboratory, Report No. 442, June 1960.

7. Culick, F. E. C.: An Integral Method for Laminar Boundary Layer Calculations: Momentum Thickness and Mass Transfer with Zero Pressure Gradient. Massachusetts Institute of Technology, Aerophysics Laboratory TR 10; July 1961. (AFOSR-1411)

8. Culick, F. E. C.: An Integral Method for Laminar Boundary Layer Calculations: Heat and Mass Transfer with Zero Pressure Gradient. Massachusetts Institute of Technology, Aerophysics Laboratory TR 16; December 1961. (AFOSR 2146)

9. King, H. H. and Talbot, L.: Effects of Mass Injection on the Drag of a Slender Cone in Hypersonic Flow. AIAA Journal, Vol. 2, No. 5, May 1964.

10. Lewis, C. H., Marchand, E. O., and Little, H. R.: Mass Transfer and First Order Boundary-Layer Effects on Sharp Cone Drag. (To be presented at AIAA 3rd Aerospace Sciences Meeting, January 24-26, 1966.)

11. Lewis, C. H. and Whitfield, J. D.: Theoretical and Experimental Studies of Hypersonic Viscous Effects, AEDC-TR-65-100, May 1965.

12. Hartree, D. R. and Womersley, J. R.: A Method for the Numerical or Mechanical Solution of Certain Types of Partial Differential Equations. Proc. Royal Soc. Series A, Vol. 161, No. 906, p. 353, August 1937.

13. Smith, A. M. O. and Clutter, D. W.: Solution of the Incompressible Laminar Boundary Layer Equations. AIAA Journal, Vol. 1, No. 9, pp. 2002-2071, September 1963.

14. Smith, A. M. O. and Clutter, D. W.: Machine Calculation of Compressible Boundary Layer. AIAA Journal, Vol. 3, No. 4, pp. 639-647, April 1965.

15. Smith, A. M. O. and Jaffe, N. A.: General Method for Solving the Nonequilibrium Boundary Layer Equations of a Dissociating Gas. AIAA paper No. 65-129, presented at AIAA 2nd Aerospace Sciences Meeting, January 25-27, 1965.

16. Probstein, R. F. and Elliott, D: The Transverse Curvature Effect in Compressible Axially Symmetric Laminar Boundary Layer Flow. Journal of the Aeronautical Sciences, March 1956.

17. Hayes, W. D. and Probstein, R. F.: Hypersonic Flow Theory. Academic Press, New York and London, p. 290, 1959.

18. Scala, S. M. and Baulknight, C. W. : Transport and Thermodynamic Properties in a Hypersonic Boundary Layer. Aerophysics Research Memo 10, General Electric Missile and Ordnance Systems Division, Technical Information Series, Document No. 58SD232, April 1958; also published in ARS Journal, Vol. 29, No. 1, January 1959, pp. 39-45.

19. JANAF Thermochemical Data Tables, Dow Chemical Company Thermal Laboratory, Midland, Michigan, 31 March 1961.

20. Clutter, D. W., Smith, A. M. O., and Jaffe, N. A.: General Method for Solving Nonequilibrium Laminar-Boundary Layer Flow of a Binary Gas. Douglas Aircraft Company Report No. LB-31616, October 16, 1964.

21. Wilke, C. R.: A Viscosity Equation for Gas Mixtures. J. Chem. Physics, Vol. 18, No. 4, April 1950, pp. 517-519.

22. Hirschfelder, J. O., Curtiss, C. F., and Bird, R.: Molecular Theory of Gases and Liquids. Chapters 7 and 8, John Wiley and Sons, New York, 1964.

23. Ames Research Staff: Equations, Tables and Charts for Compressible Flow. NACA 1135, 1953.

24. Amdur, I. and Mason, E. A.: Properties of Gases at Very High Temperatures. Physics of Fluids, Vol. 1, No. 5, September 1958.

25. Thomas, M.: The High Temperature Transport Properties of Carbon Dioxide. Douglas Report SM-37790, July 1960.

26. Svehla, R. A.: Thermodynamic and Transport Properties for the Hydrogen-Oxygen System. NASA SP-3011, 1964.

27. Eucken, A.: Physik 2. Vol. 14, pp. 324-332, 1913.

28. Moore, J. A. and Pallone, A.: Similar Solutions to the Laminar Boundary Layer Equations for Nonequilibrium Air. AVCO Technical Memorandum RAD-TM-62-59, July 1962.

29. Monchick, L.: Collision Integrals for the Exponential Repulsive Potential. Physics of Fluids, Vol. 6, No. 2, 1959.

30. Collatz, L.: The Numerical Treatment of Differential Equations. Third Edition, Springer-Verlag, Berlin, 1960.

31. Clutter, D.W. and Smith, A.M.O.: Solution of the General Boundary Layer Equations for Compressible Laminar Flow, Including Transverse Curvature, Report No. LB 31088, February 15, 1963; revised October 1, 1964

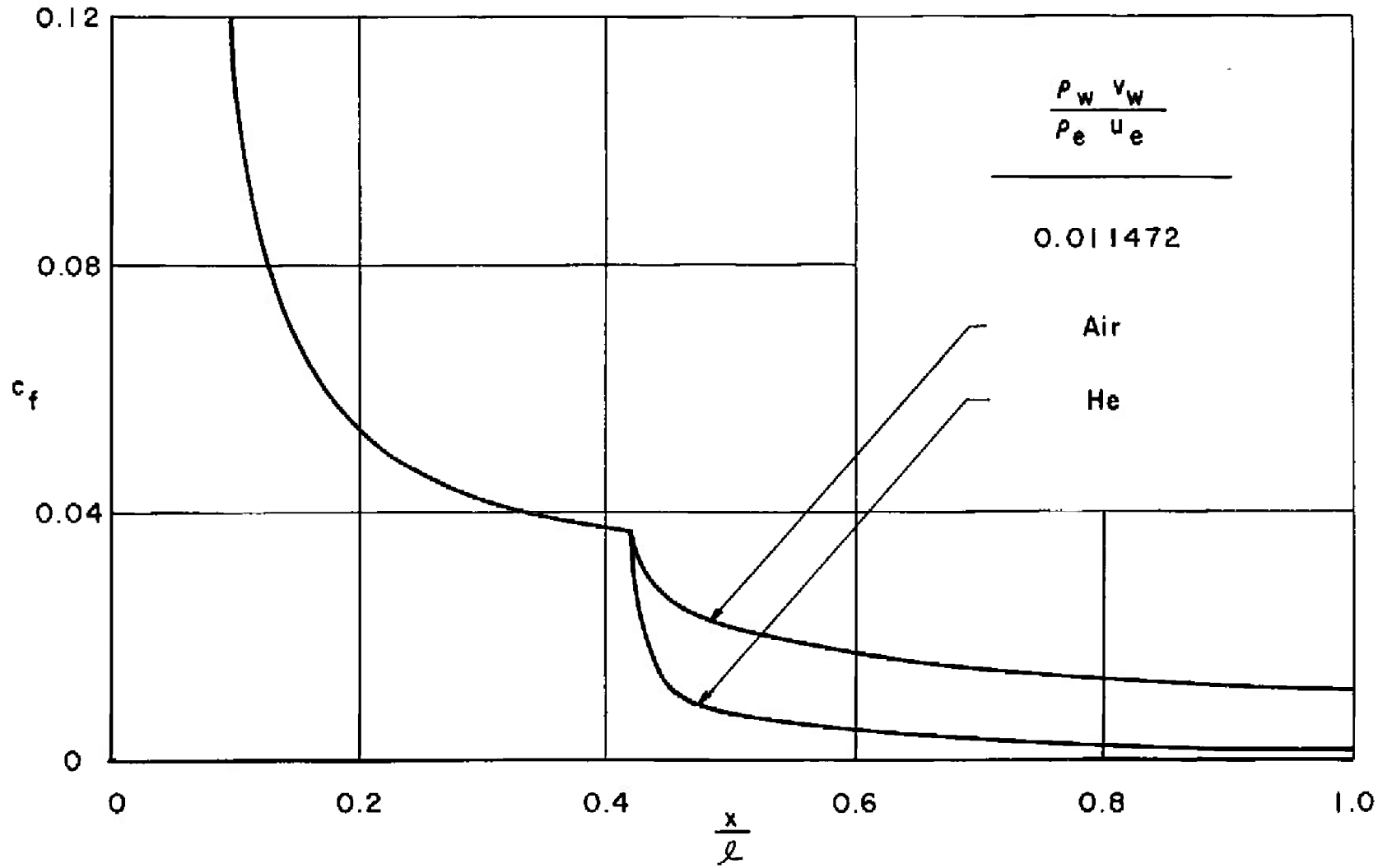

Figure 4. - Comparison of Boundary Layer Parameters for He and Air Injection, Neglecting TVC. (a) Coefficient of Skin Friction

AEDC-TR-66-183

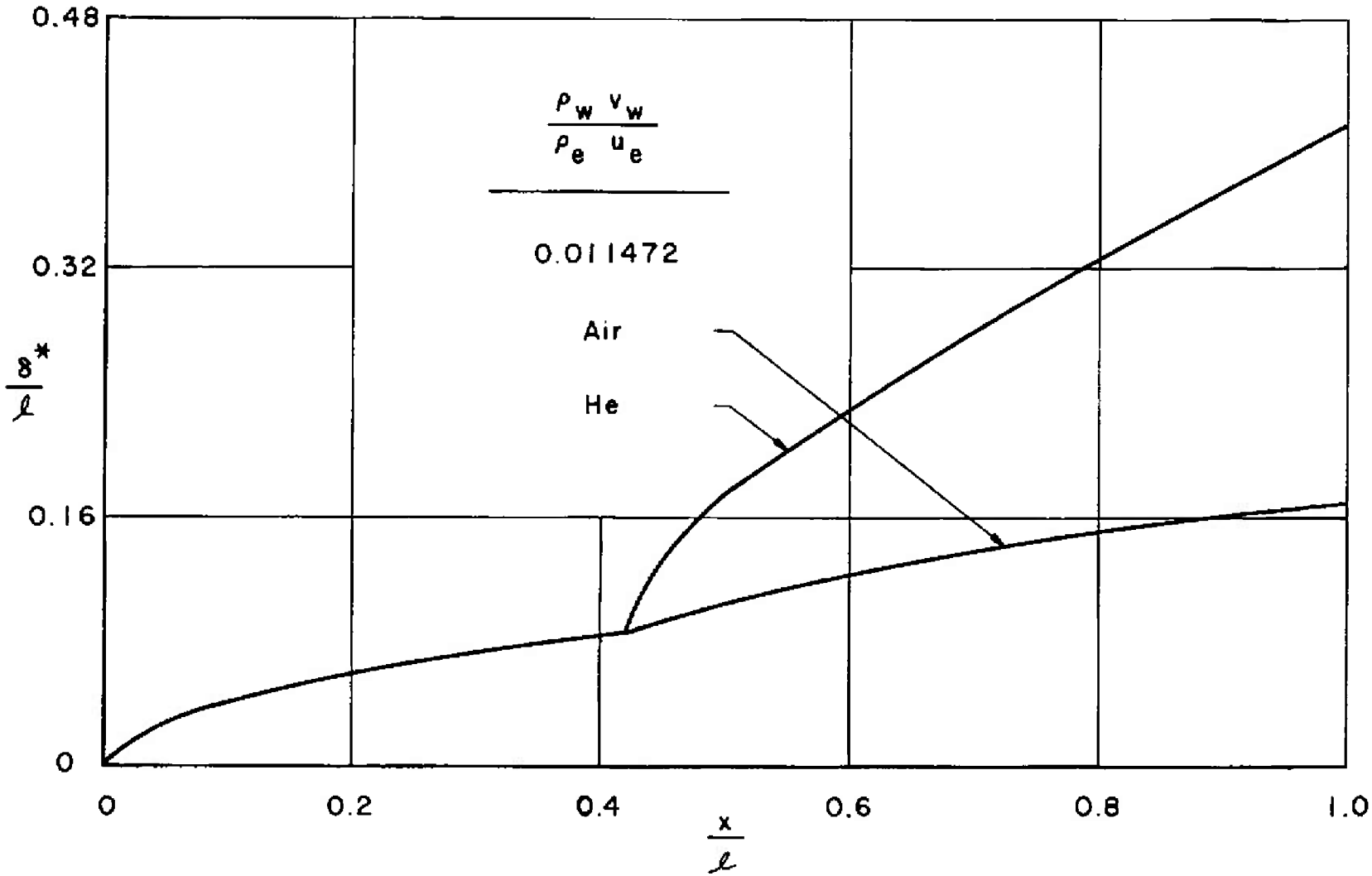

Figure 4. - Concluded. (b) Displacement Thickness

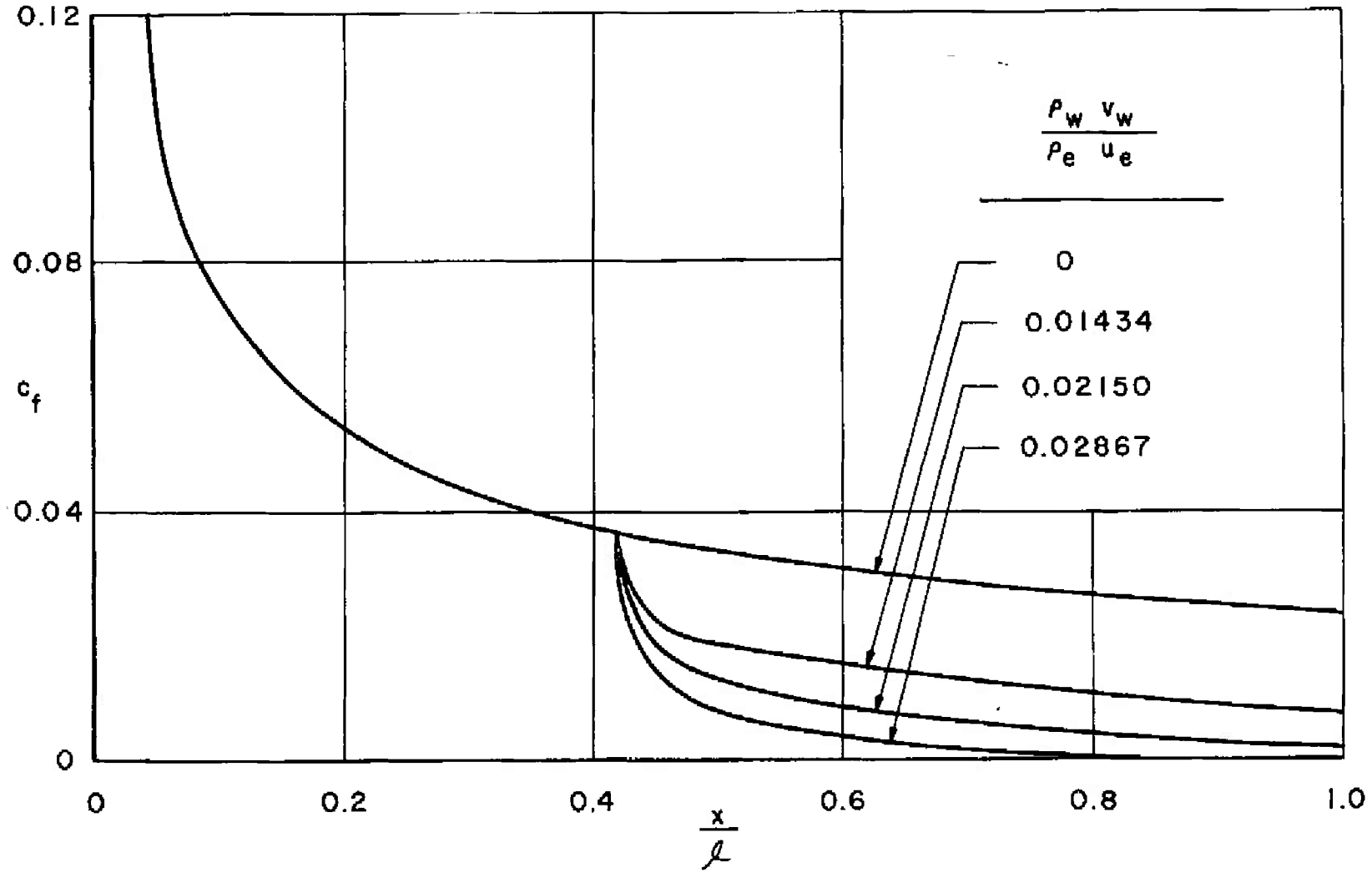

Figure 5. - Boundary Layer Parameters for Air Injection, Neglecting TVC. (a) Coefficient of Skin Friction

AEDC-TR-66-183

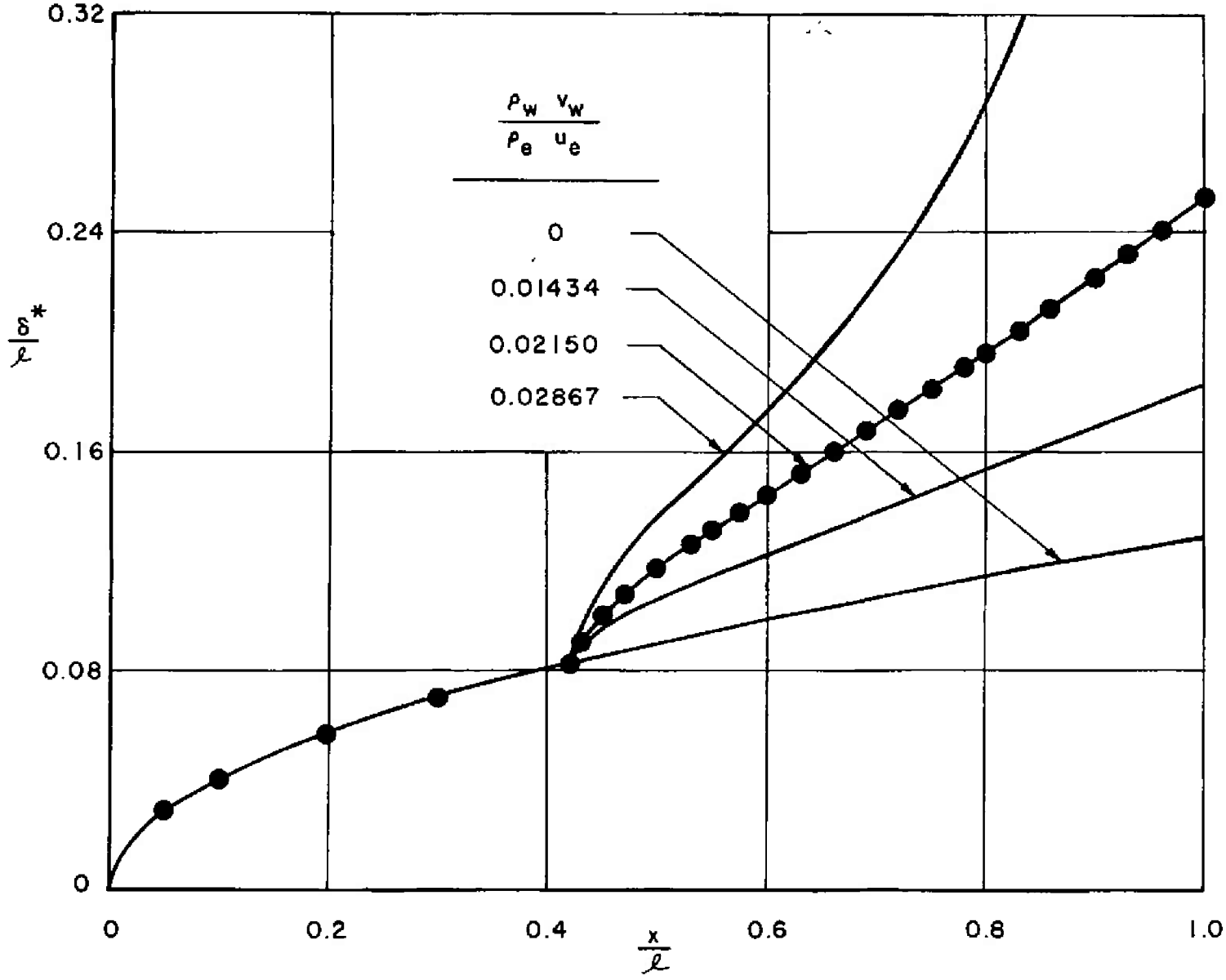

Figure 5. - Concluded. (b) Displacement Thickness

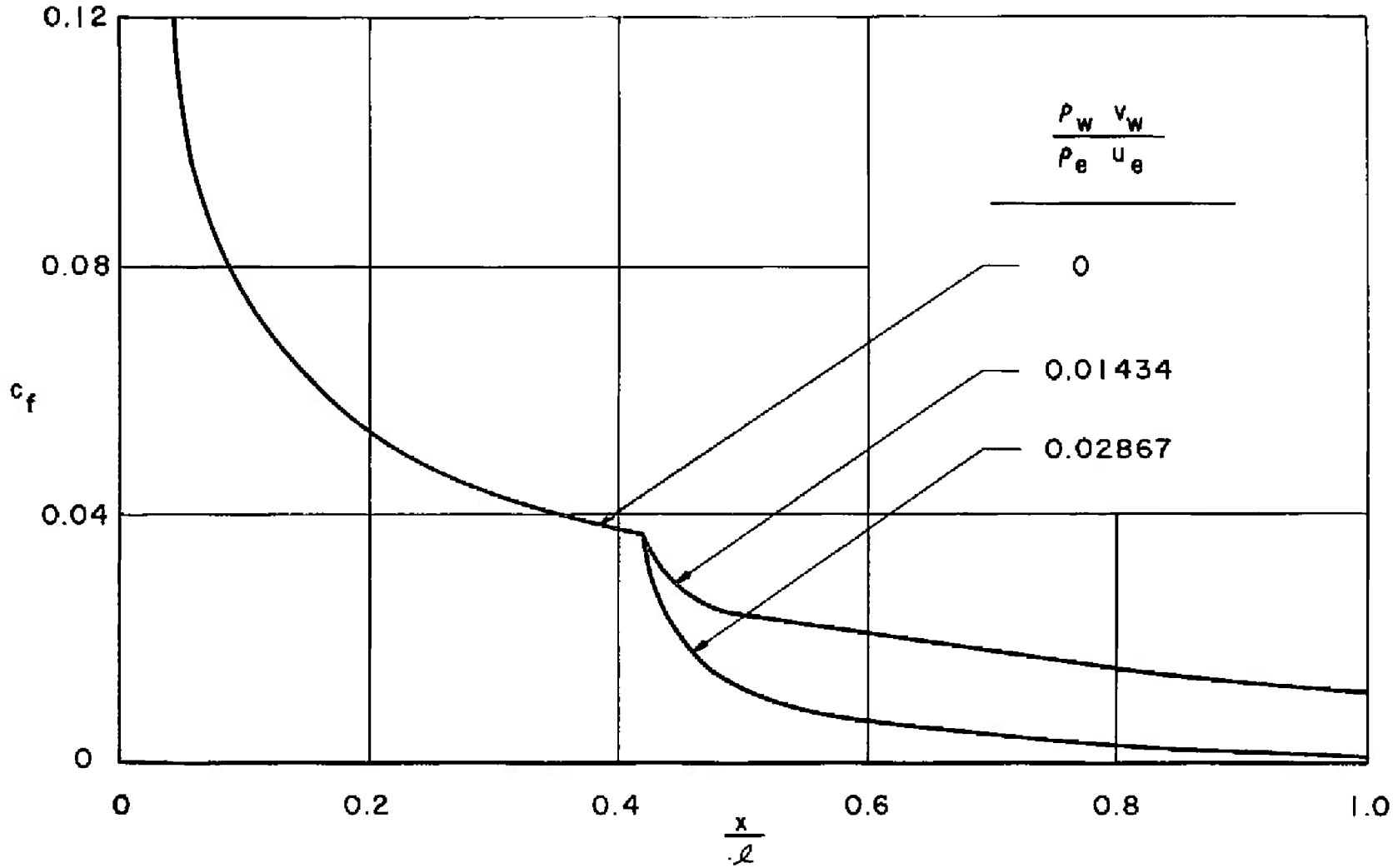

Figure 6. - Boundary Layer Parameters for Ar Injection, Neglecting TVC. (a) Coefficient of Skin Friction

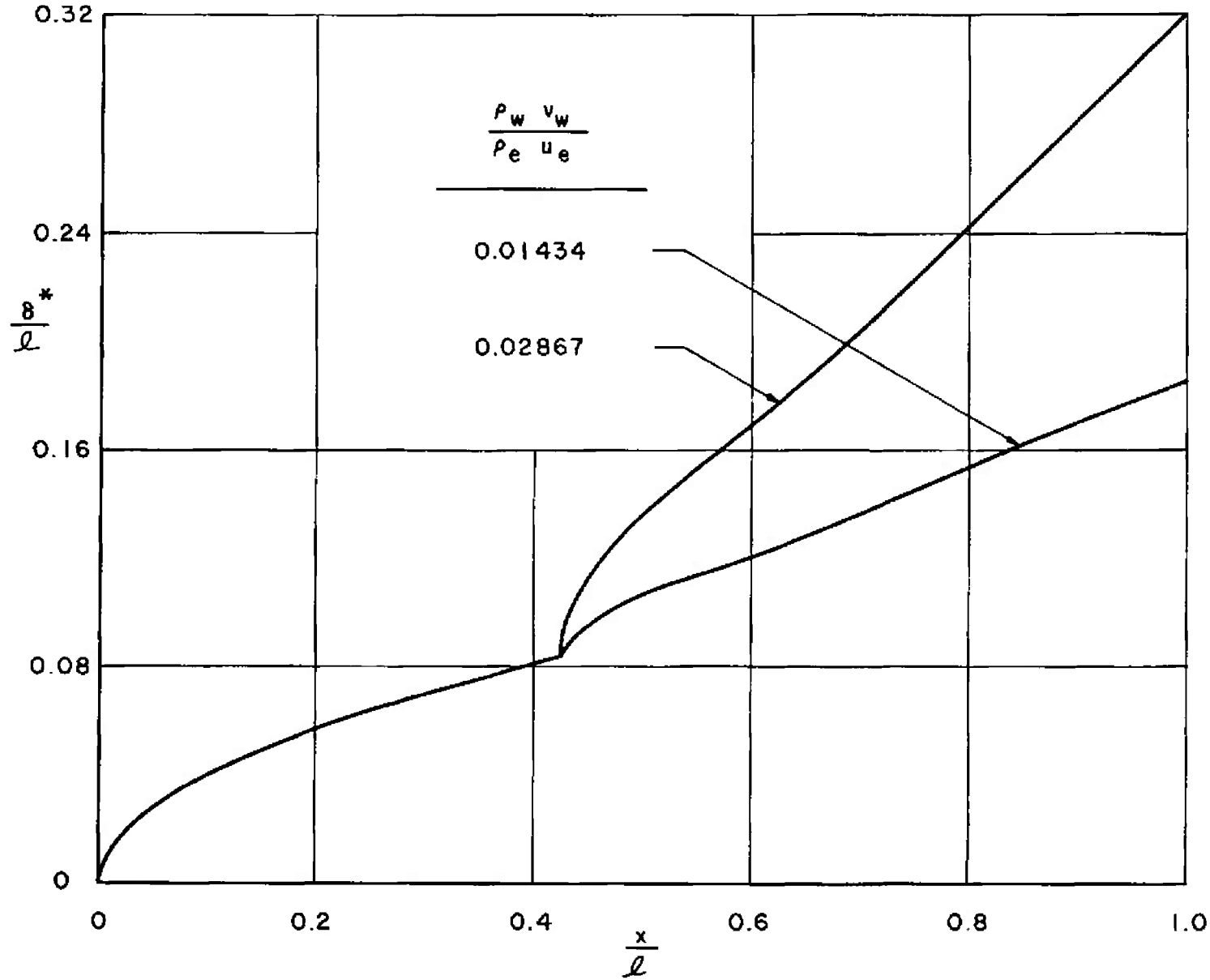

Figure 6. - Concluded. (b) Displacement Thickness

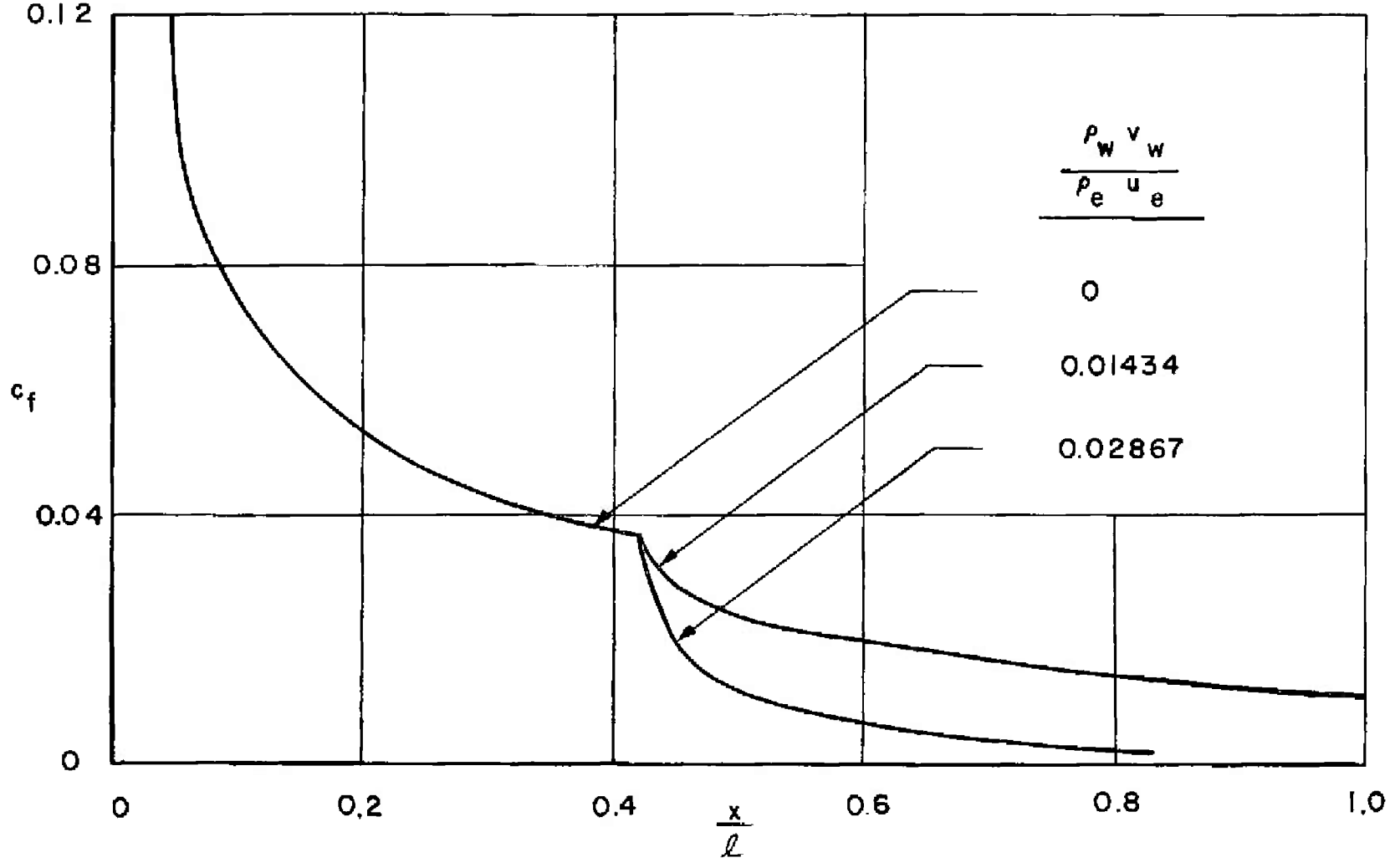

Figure 7. - Boundary Layer Parameters for CO_2 Injection, Neglecting TVC. (a) Coefficient of Skin Friction

AEDC-TR-66-183

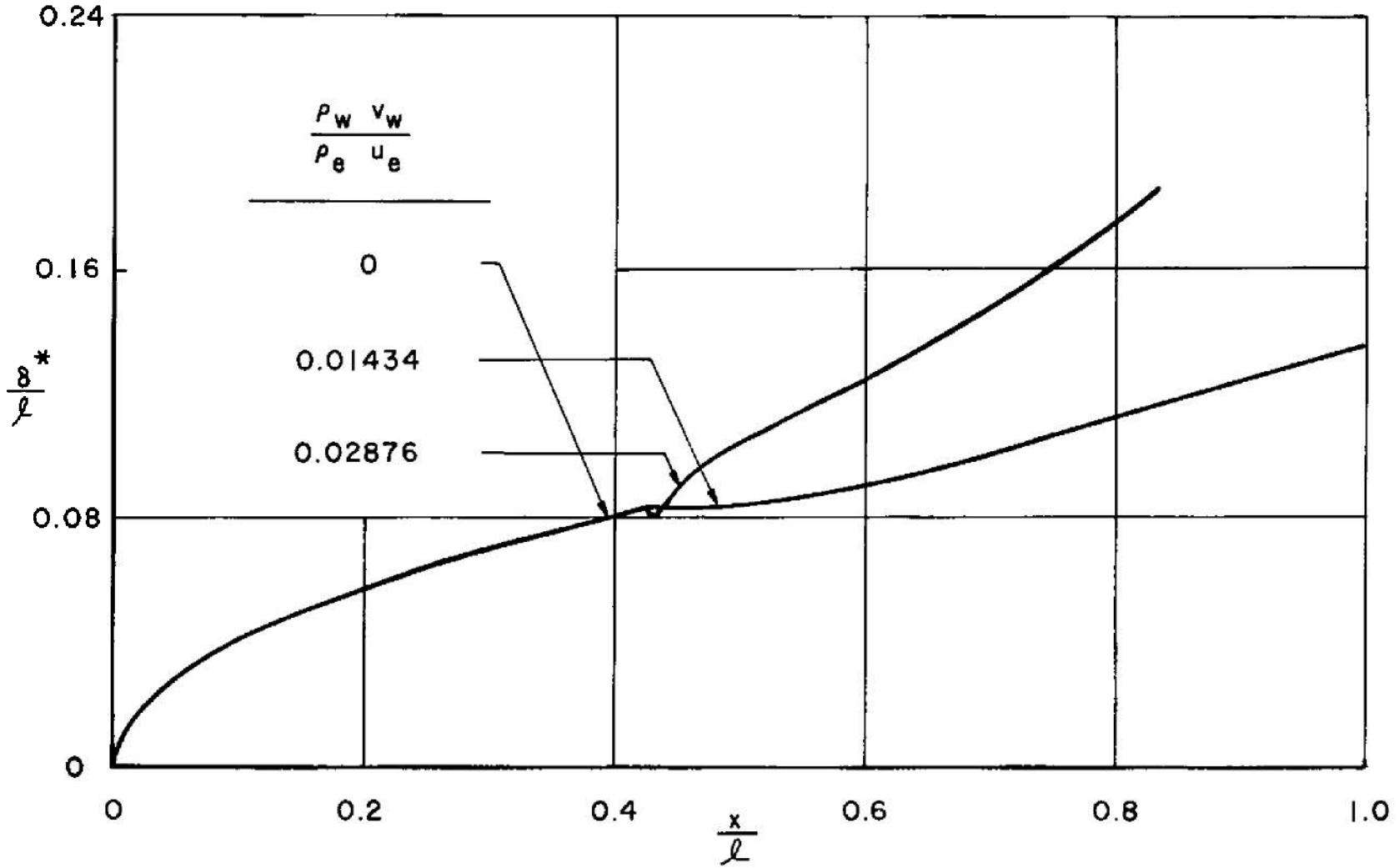

Figure 7. - Concluded. (b) Displacement Thickness

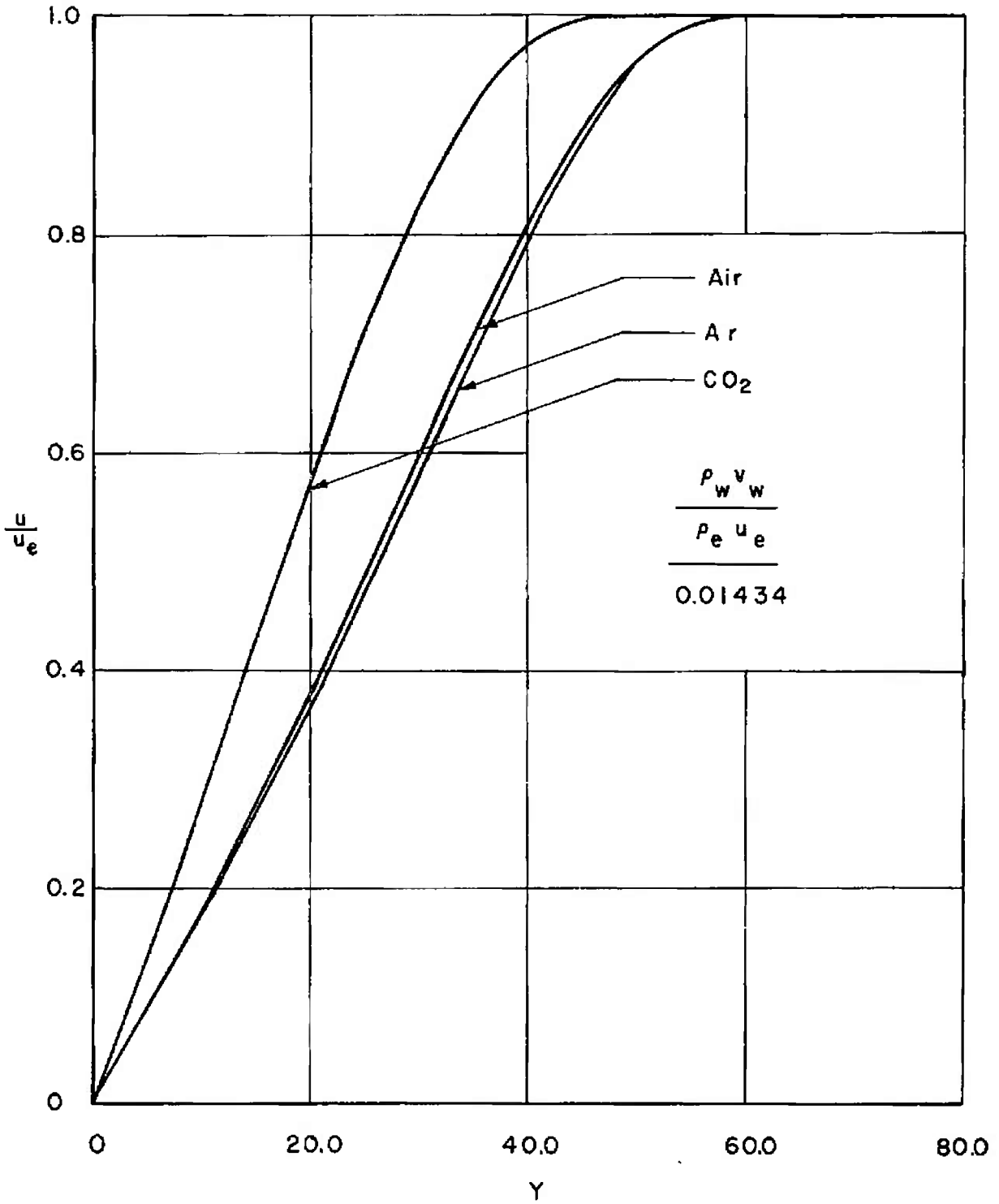

Figure 8. - Comparison of Boundary Layer Profiles at $x/\ell = 0.75$ Neglecting TVC. (a) Dimensionless Velocity Profiles

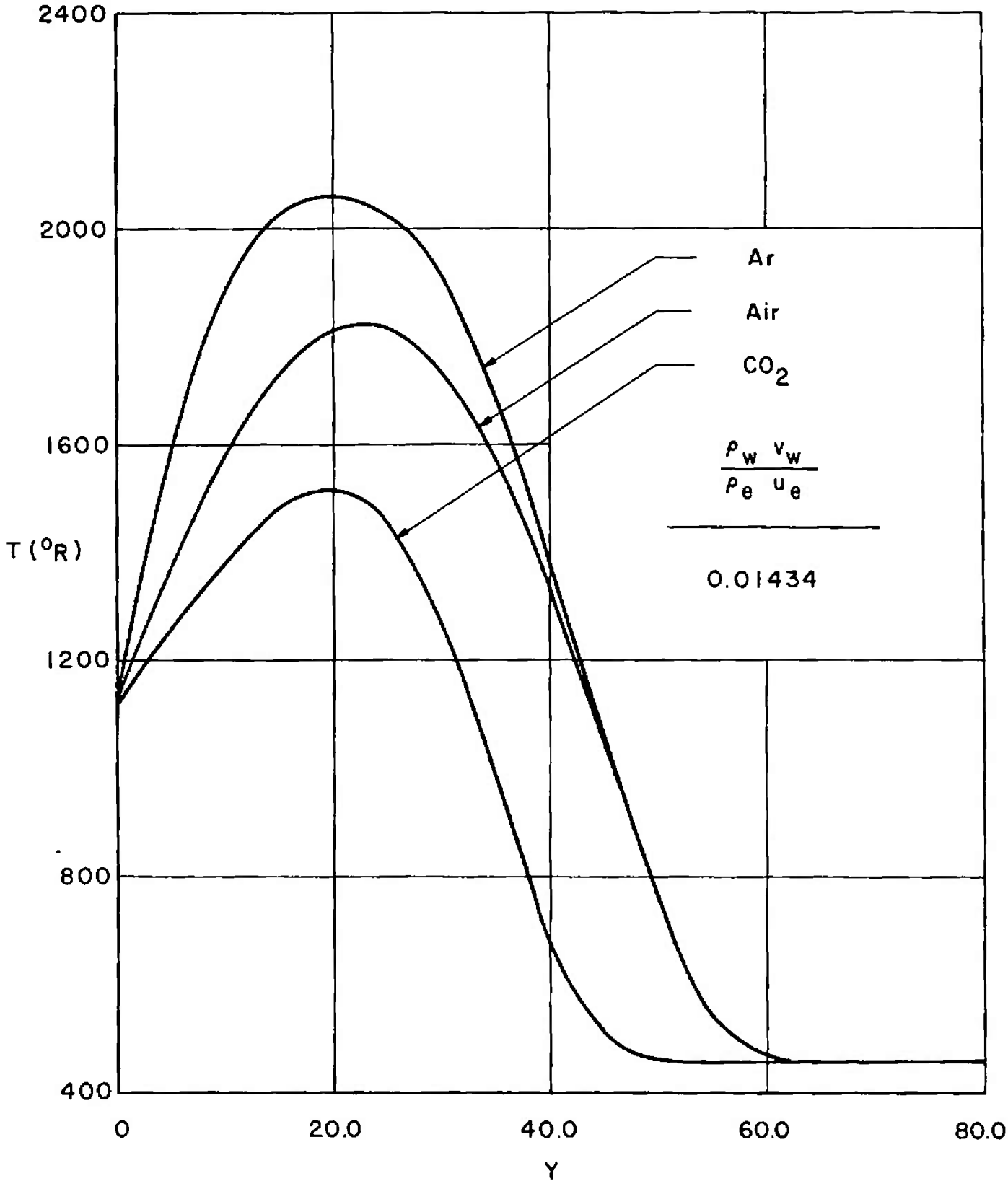

Figure 8. - Continued. (b) Temperature Profiles

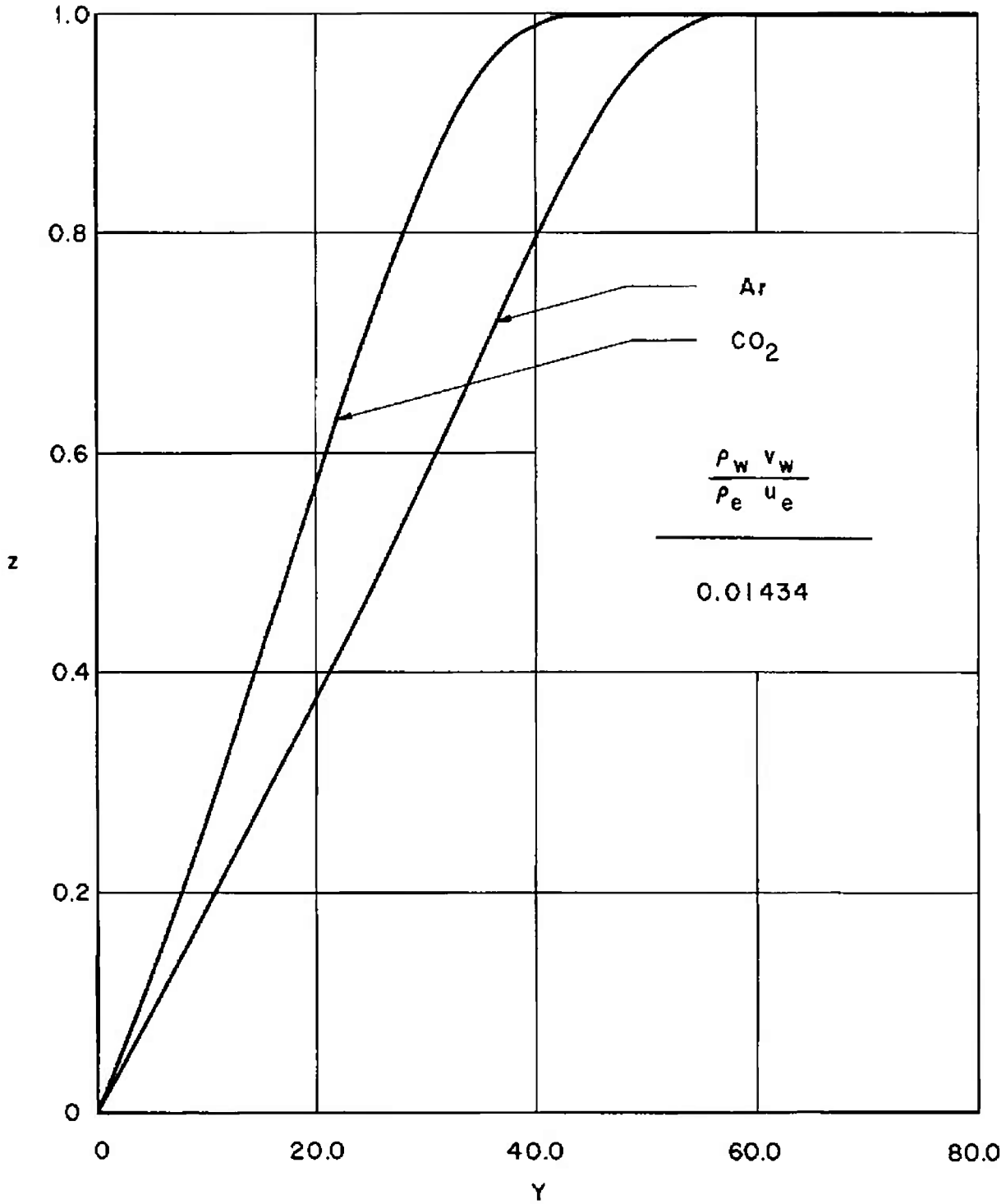

Figure 8. - Concluded. (c) Mass Fraction Profiles

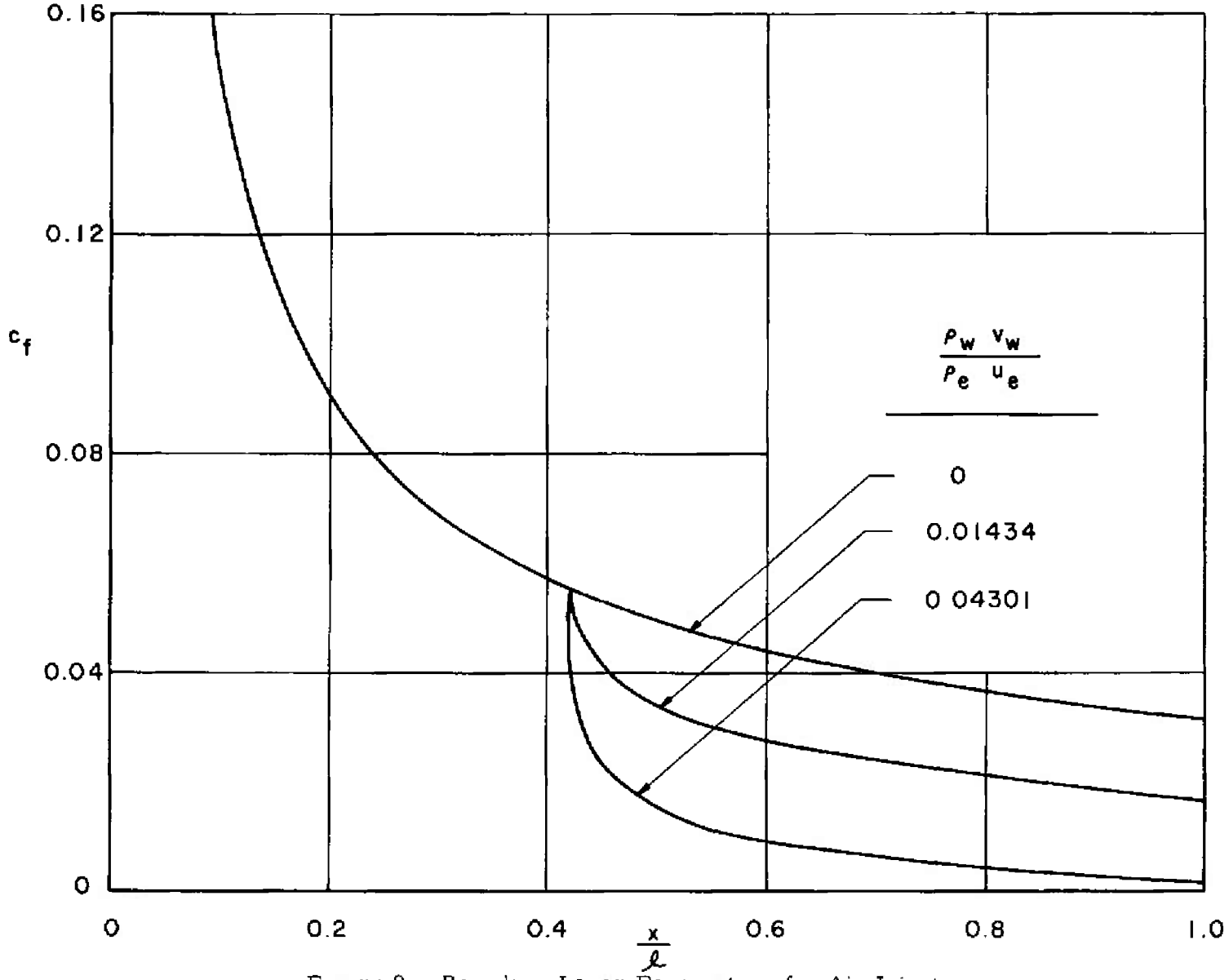

Figure 9. - Boundary Layer Parameters for Air Injection, Including TVC. (a) Coefficient of Skin Friction

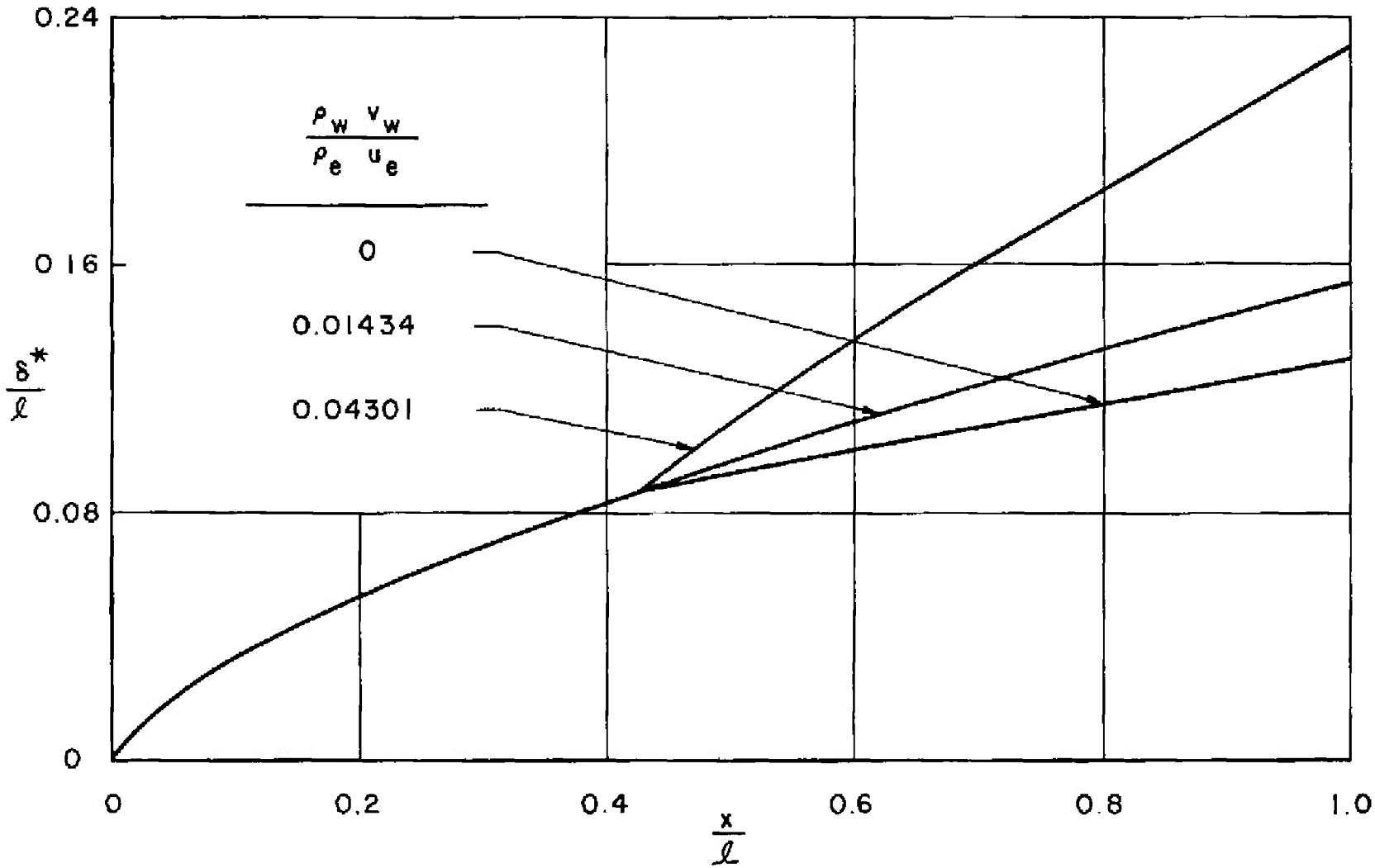

Figure 9. - Concluded. (b) Displacement Thickness

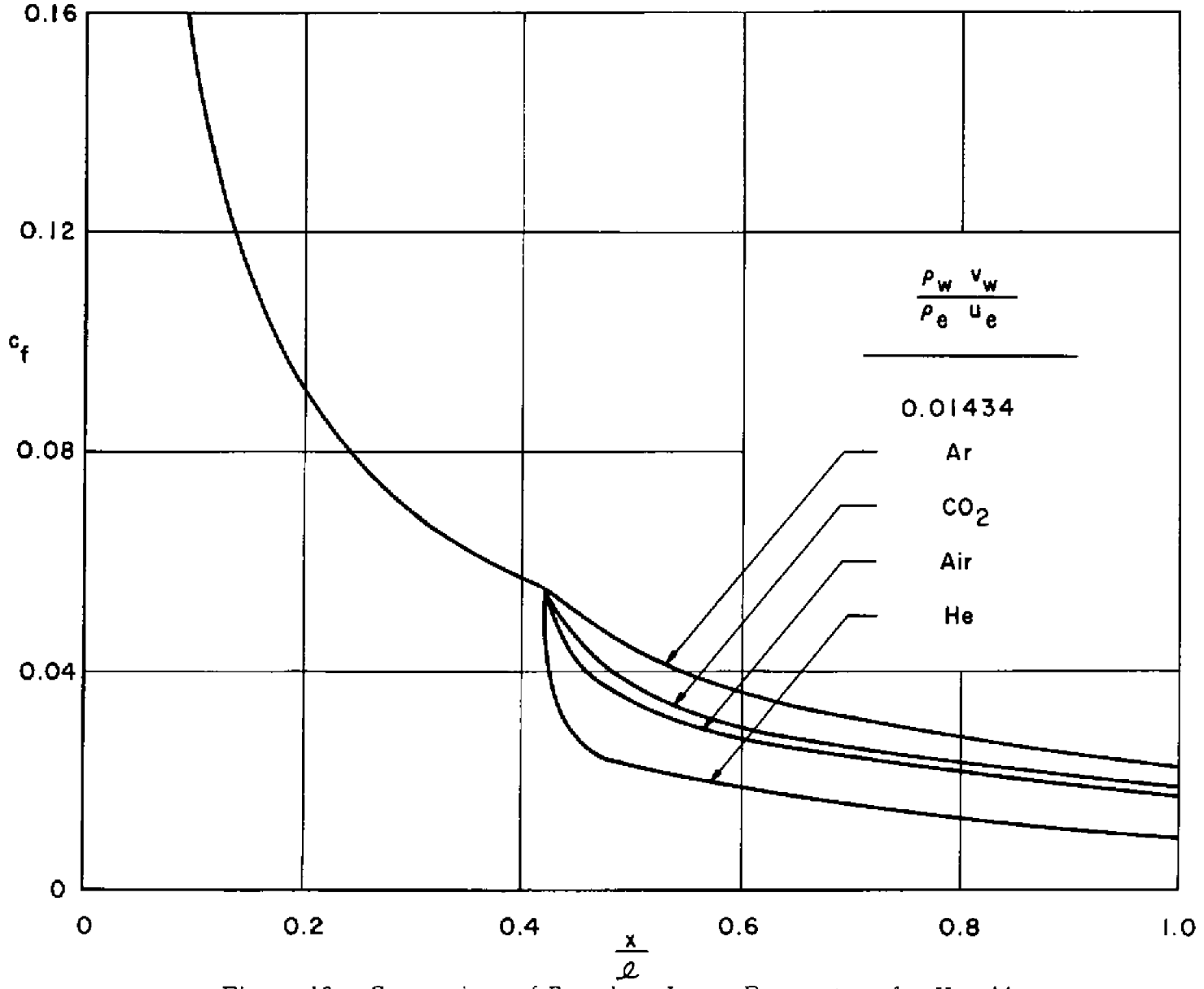

Figure 10. - Comparison of Boundary Layer Parameters for He, Air, Ar, and CO_2 Injection, Including TVC. (a) Coefficient of Skin Friction

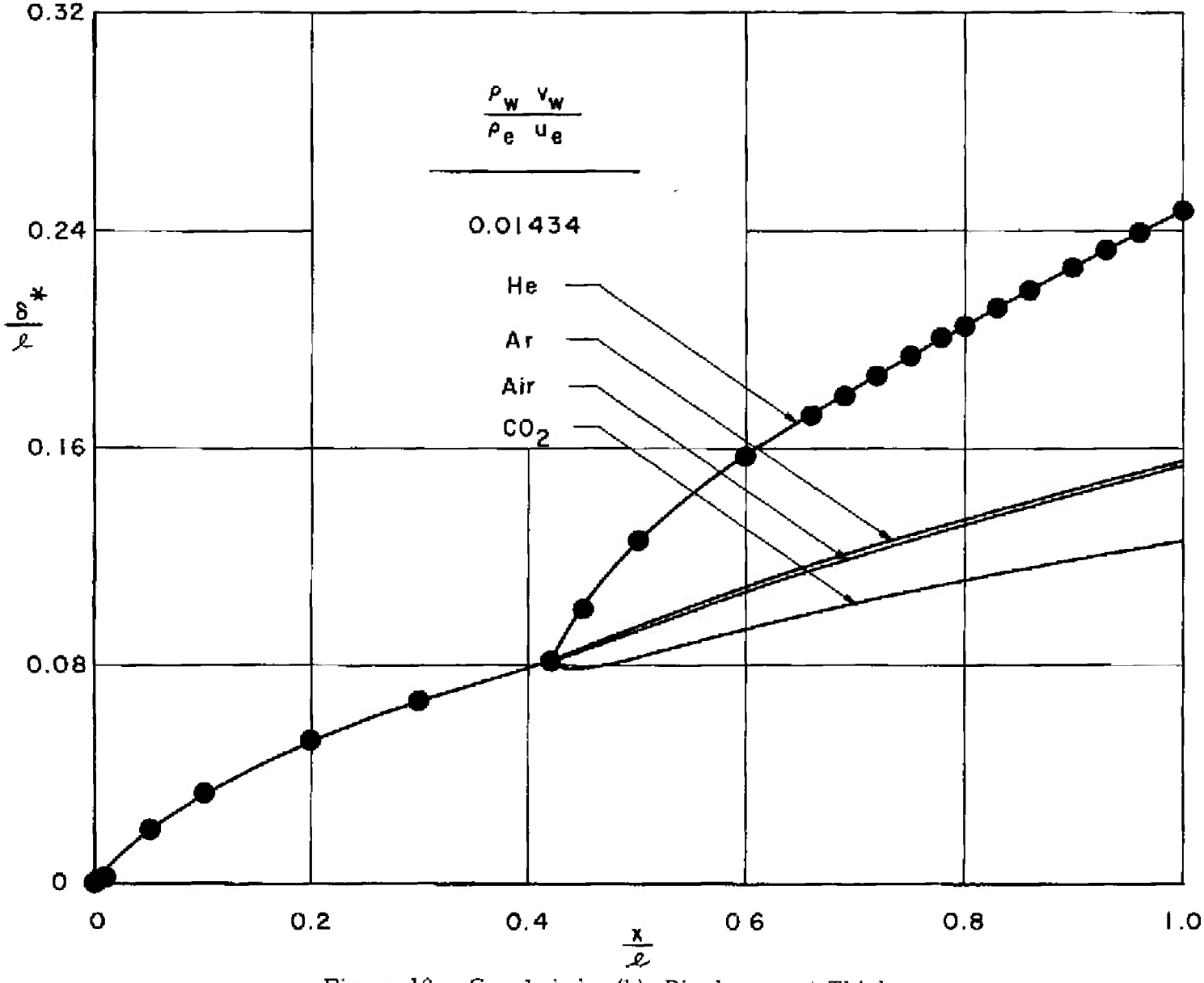

Figure 10. - Concluded. (b) Displacement Thickness

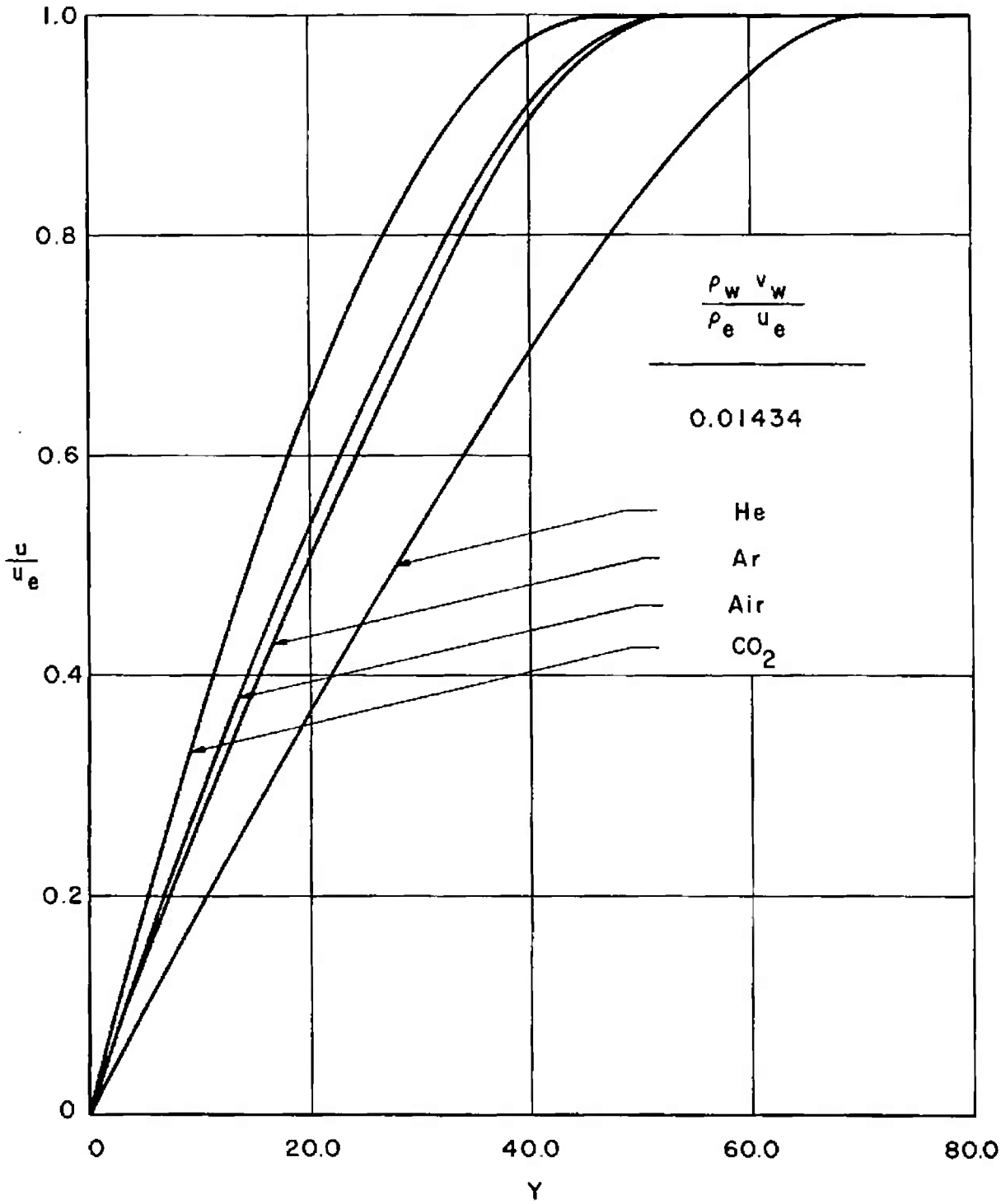

Figure 11. - Comparison of Boundary Layer Profiles at $x/\ell = 0.75$, Including TVC. (a) Dimensionless Velocity Profiles

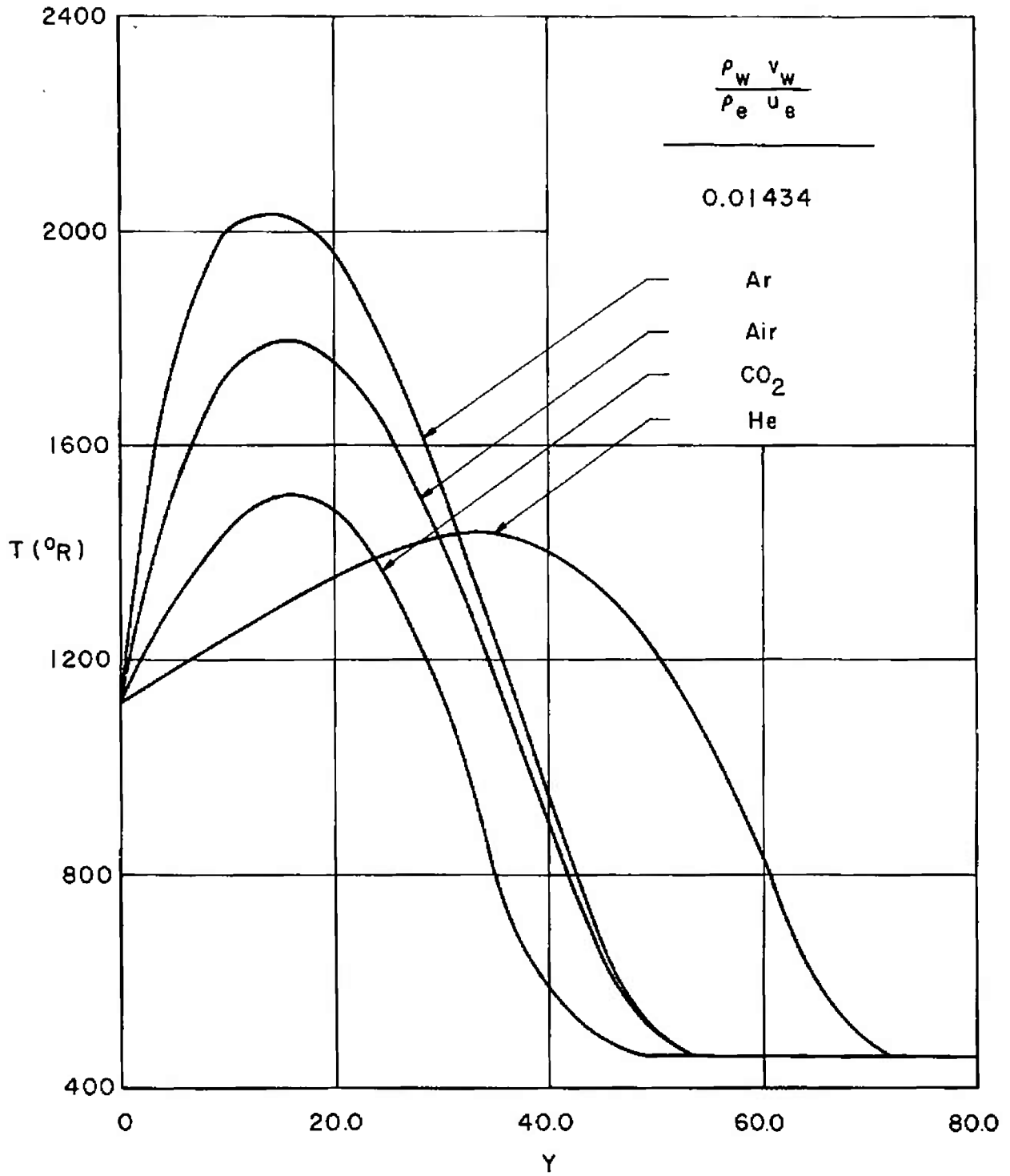

Figure 11. - Continued. (b) Temperature Profiles

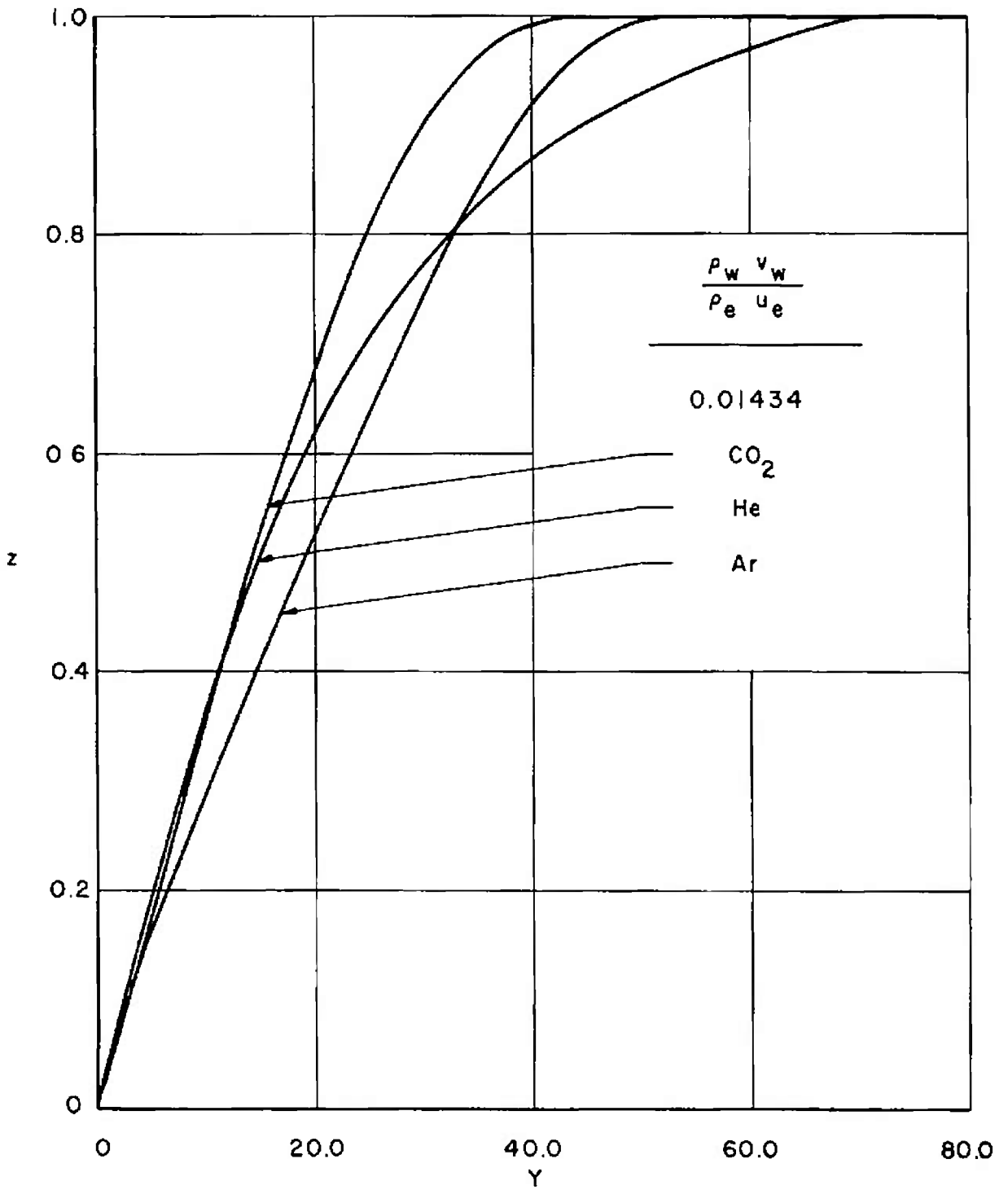

Figure 11. - Concluded. (c) Mass Fraction Profiles

Security Classification

DOCUMENT CONTROL DATA - R&D

(Security classification of title, body of abstract and indexing annotation must be entered when the overall report is classified)

1 ORIGINATING ACTIVITY (Corporate author)
Douglas Aircraft Div., a Div. of Douglas Aircraft Co., Inc., Long Beach, California

2a REPORT SECURITY CLASSIFICATION
UNCLASSIFIED

2b GROUP
N/A

3 REPORT TITLE
SOLUTION TO THE BINARY DIFFUSION LAMINAR BOUNDARY LAYER EQUATIONS INCLUDING THE EFFECT OF SECOND-ORDER TRANSVERSE CURVATURE

4 DESCRIPTIVE NOTES (Type of report and inclusive dates)
N/A

5 AUTHOR(S) (Last name, first name, initial)
Jaffe, N. A., Lind, R. C., and Smith, A. M. O., Douglas Aircraft Div.

6 REPORT DATE	7a TOTAL NO OF PAGES	7b NO OF REFS
February 1967	85	31

8a CONTRACT OR GRANT NO
AF40(600)-1000

b PROJECT NO 8953

c Program Element 62405334

d Task 895303 and 895306

9a ORIGINATOR'S REPORT NUMBER(S)
AEDC-TR-66-183

9b OTHER REPORT NO(S) (Any other numbers that may be assigned this report)
LB-32613

10 AVAILABILITY/LIMITATION NOTICES Distribution of this document is unlimited. Available in DDC.

11 SUPPLEMENTARY NOTES Work was conducted under Purchase Order 5A-9405 from ARO, Inc., Contract Operator, AEDC

12 SPONSORING MILITARY ACTIVITY
Arnold Engineering Development Center, Air Force Systems Command, Arnold Air Force Station, Tenn.

13 ABSTRACT

This report presents a numerical method for solving the binary diffusion laminar boundary-layer equations. The differential equations of continuity, momentum, energy, and species diffusion are solved simultaneously for two-dimensional or axisymmetric flow. For the case of axisymmetric flow the second-order transverse curvature terms appearing in the equations are retained. Relations for mixture fluid properties as functions of local conditions in the boundary layer are developed and used in obtaining solutions to the equations. The mixtures considered in this investigation are He - air, Ar - air, and CO_2 - air. Solutions to the equations are given for flow of a pure air free stream over a 9^o half angle cone at a free stream Mach number of 10 and free stream Reynolds number, based on cone slant length of 940. The initial section of the cone is solid and mass injection is initiated at a location downstream of the tip. Results are presented and compared for calculations both including and neglecting the second-order transverse curvature effect.

DD FORM 1 JAN 64 1473

Security Classification

14 KEY WORDS	LINK A		LINK B		LINK C	
	ROLE	WT	ROLE	WT	ROLE	WT
binary diffusion						
laminar boundary layer						
differential equations						
solutions						
axisymmetric flow						
fluid mixing properties						
gas mixtures						
hypersonic flow						
mass injection						
conical bodies						

INSTRUCTIONS

1. ORIGINATING ACTIVITY: Enter the name and address of the contractor, subcontractor, grantee, Department of Defense activity or other organization *(corporate author)* issuing the report.

2a. REPORT SECURITY CLASSIFICATION: Enter the overall security classification of the report. Indicate whether "Restricted Data" is included. Marking is to be in accordance with appropriate security regulations.

2b. GROUP: Automatic downgrading is specified in DoD Directive 5200.10 and Armed Forces Industrial Manual. Enter the group number. Also, when applicable, show that optional markings have been used for Group 3 and Group 4 as authorized.

3. REPORT TITLE: Enter the complete report title in all capital letters. Titles in all cases should be unclassified. If a meaningful title cannot be selected without classification, show title classification in all capitals in parenthesis immediately following the title.

4. DESCRIPTIVE NOTES: If appropriate, enter the type of report, e.g., interim, progress, summary, annual, or final. Give the inclusive dates when a specific reporting period is covered.

5. AUTHOR(S): Enter the name(s) of author(s) as shown on or in the report. Enter last name, first name, middle initial. If military, show rank and branch of service. The name of the principal author is an absolute minimum requirement.

6. REPORT DATE: Enter the date of the report as day, month, year; or month, year. If more than one date appears on the report, use date of publication.

7a. TOTAL NUMBER OF PAGES: The total page count should follow normal pagination procedures, i.e., enter the number of pages containing information.

7b. NUMBER OF REFERENCES: Enter the total number of references cited in the report.

8a. CONTRACT OR GRANT NUMBER: If appropriate, enter the applicable number of the contract or grant under which the report was written.

8b, 8c, & 8d. PROJECT NUMBER: Enter the appropriate military department identification, such as project number, subproject number, system numbers, task number, etc.

9a. ORIGINATOR'S REPORT NUMBER(S): Enter the official report number by which the document will be identified and controlled by the originating activity. This number must be unique to this report.

9b. OTHER REPORT NUMBER(S): If the report has been assigned any other report numbers *(either by the originator or by the sponsor)*, also enter this number(s).

10. AVAILABILITY/LIMITATION NOTICES: Enter any limitations on further dissemination of the report, other than those imposed by security classification, using standard statements such as:

(1) "Qualified requesters may obtain copies of this report from DDC."

(2) "Foreign announcement and dissemination of this report by DDC is not authorized."

(3) "U. S. Government agencies may obtain copies of this report directly from DDC. Other qualified DDC users shall request through _____."

(4) "U. S. military agencies may obtain copies of this report directly from DDC. Other qualified users shall request through _____."

(5) "All distribution of this report is controlled. Qualified DDC users shall request through _____."

If the report has been furnished to the Office of Technical Services, Department of Commerce, for sale to the public, indicate this fact and enter the price, if known.

11. SUPPLEMENTARY NOTES: Use for additional explanatory notes.

12. SPONSORING MILITARY ACTIVITY: Enter the name of the departmental project office or laboratory sponsoring *(paying for)* the research and development. Include address.

13 ABSTRACT. Enter an abstract giving a brief and factual summary of the document indicative of the report, even though it may also appear elsewhere in the body of the technical report. If additional space is required, a continuation sheet shall be attached.

It is highly desirable that the abstract of classified reports be unclassified. Each paragraph of the abstract shall end with an indication of the military security classification of the information in the paragraph, represented as *(TS), (S), (C), or (U)*

There is no limitation on the length of the abstract. However, the suggested length is from 150 to 225 words.

14. KEY WORDS: Key words are technically meaningful terms or short phrases that characterize a report and may be used as index entries for cataloging the report. Key words must be selected so that no security classification is required. Identifiers, such as equipment model designation, trade name, military project code name, geographic location, may be used as key words but will be followed by an indication of technical context. The assignment of links, rules, and weights is optional.